NASA
Technical
Paper
2390

1984

Flow Rates and Pressure Profiles for One to Four Axially Alined Borda Inlets

Robert C. Hendricks
and T. Trent Stetz

Lewis Research Center
Cleveland, Ohio

NASA
National Aeronautics
and Space Administration

**Scientific and Technical
Information Branch**

Summary

Choked flow rate and pressure profile data were taken on sequential, axially alined inlets of the Borda type. The configurations consisted of two to four inlets spaced 0.8 and 30 diameters apart. Reference data were taken for the limiting case of a single Borda inlet.

At a spacing of 30 diameters the reduced flow rate appeared to follow the simple empirical relation

$$G_r/G_{r,1} = N^{-b}$$

where $G_{r,1}$ is the reduced flow rate for a single inlet; N is the number of inlets; and b, which is weakly temperature dependent, is approximately 0.4. The relation is in reasonable agreement with an analysis of the N-inlet configuration. At a spacing of 30 diameters the pressure profiles dropped sharply at the entrance and partially recovered within each inlet somewhat independently of N. Jetting through the last Borda was common at low temperatures.

At a spacing of 0.8 diameter fluid jetting was prevalent at low temperatures for each configuration studied and flow rates were the same as that for a single inlet.

Introduction

Contoured inlet configurations are common to heat transfer devices and fluid machinery components. Most inlet configurations consist of sequential inlets. Labyrinth and step seals, for example, have inlet configurations that consist of two or more sequential inlets. The details of the flow dynamics in these configurations are not well understood in many cases, as was encountered in reference 1, where the flow appeared to separate and jet through the third-stage length in the maximum-clearance channel when the seal was placed in the fully eccentric position.

The unusual results of reference 1 provoked a series of choked-flow tests with single and multiple sharp-edge orifices and Borda inlets. These studies (refs. 2 to 8) demonstrated that jetting could occur over a wide range of fluid state conditions. The tubes with single sharp-edge orifice and Borda inlets (refs. 2, 3, 4, and 6) provided a few details about flow jetting. Flow jetting was, however, found to be inhibited (1) by high inlet stagnation temperatures ($T_r > 1$) and by low pressures to a lesse extent; (2) by a high length-to-diameter ratio L/D at on extreme and a low L/D at the other extreme; (3) by th saturated liquid locus, where the "liquid like" jet tende to reattach because of rapid vapor release; and (4) b tube roughness. These tests established that jetting coul occur in a single inlet passage.

In references 5, 7, and 8 the effects of four sequentia axially alined Borda and orifice inlets were investigated a a first look at discontinuities of sequential inlets. Wate table flow visualization studies of these inlets indicate that, for $L/D < 1$, jetting could occur. For $L/D < 20$ th flow appeared to be nearly independent of the reservoi Flow instabilities were pronounced for the rang $1 < L/D < 10$. When cryogenic fluids were used, th experimental tests with the four Borda and four orific axially alined inlets demonstrated that for a spacing c nominally 30 L/D the flow was nearly independent of th upstream inlets and reservoirs. Jetting did occur in th fourth inlet at lower inlet stagnation temperatures. At spacing of nominally 0.7 L/D, jetting was commonpla and the flow appeared to be independent of th configuration.

A few other studies have been done on axially aline sequential inlets. One such study is that of Boscol Martin, and Donnis (ref. 9), who were mainly intereste in the improvement of flowmeters. Benckert an Wachter (ref. 10) recently presented a thorough study c the stability of see-through and leaved labyrinth seal Iwatsubo (ref. 11) also studied the stability of flows labyrinth seal cavities. His results seem to be nearly tl analytic complement to the experimental work Benchert and Wachter (ref. 10). Komotori and Mori (re 12) studied the isentropic expansion of a perfect g through labyrinth seals. These studies serve as limiti cases and guides to experimentation and analysis.

In these latter references (9 to 12) the working-flu states are either incompressible liquid or gas, and tl range of fluid conditions usually encountered with cry gens is not considered. In references 2, 3, 4, and 6 sing inlets were studied; and in references 5, 7, and 8, fo sequential inlets over a range of conditions. However, r correspondence has been made between these results a the characteristics of two or three sequential inlets.

The nature of the flow rates and pressure distributio in four sequential inlets of the Borda type at spacings

0.8 and 30 diameters is determined herein over a wide range of fluid state conditions.

Symbols

C_f flow coefficient
D diameter of inlet
G mass flow rate
G^* flow-normalizing parameter, 6010 g/cm^2 s for nitrogen
H enthalpy
L spacing
l length of Borda inlet
N number of inlets
P pressure
S entropy
T temperature
V specific volume
ρ density, $1/V$

Subscripts:

c thermodynamic critical
e exit
i ith sequential inlet
m maximum
r reduced by normalizing parameter
0 stagnation, or reference
1 case for $N=1$, the single inlet

Apparatus and Instrumentation

The flow facility, a blowdown type, basically described in reference 14 and shown in figure 1, was modified to accommodate the sequential inlet configurations (refs. 5 and 7). The working fluid was nitrogen. Borda inlets with L/D of 1.9 were designed to be similar to those used in reference 2. Spacers of 15.2 cm (6.0 in.) and 1.03 cm (0.407 in.) provided two fixed spacings of 30 and 0.8 diameter, respectively. Schematics of the N-sequential-Borda-inlet configurations with these spacings are illustrated in figure 2. This figure also provides details of the Borda inlet geometry and pressure-tap locations. A detailed photograph of the Borda inlet is given in figure 3. The configuration was "sandwiched" between inlet and outlet flange adaptors to accommodate the multiple lengths. The multiple surfaces were satisfactorily sealed by thin Mylar gaskets between flat faces. An example of the test installation is given in figure 4.

The pressure data were recorded as described in references 5 and 13. Again the working fluid was nitrogen and the reduced temperature ranged from 0.68 to 2.5 (liquid to gas), with the reduced pressure to 2.5.

Analysis

The treatment of the simplest set of sequential inlets is quite complicated. The expansion involves fluid separation, jetting, oscillations, turbulence, vortex streets, dissipation—and for stagnation entropy less than thermodynamic critical entropy, a change of phase. Sequential expansions are perturbed in a complicated way and are quite difficult to assess either experimentally or theoretically. For the analysis there are several unknowns, such as the pressure ratio across the first inlet and the choking conditions. Consequently, even the most idealized treatment is not closed and requires some iteration.

To treat the sequential inlet problem analytically, we assumed the entire process to be adiabatic with a series of isentropic expansions across each inlet followed by an isobaric recovery in a "mixing chamber" to the adiabatic locus (ref. 5). This procedure was quite similar to the approach given by Komotori and Mori (ref. 12) for flow through labyrinth seals.

The governing equations, described in reference 5, can be written as

$$G^2 = 2C_f \rho_i^2 (H_0 - H_i)$$

with the following constraints:

Isentropic

$$S_0(P_0, T_0)\Big|_i = S_e(P_e, T_e)\Big|_i$$

Isobaric

$$P_{e,i} = P_{0,i+1}$$

Critical flow (choked)

$$G_m^2 \left(\frac{dV}{dP}\right)_e \Bigg|_{i=N} = -1$$

where

$$G_m^2 = \frac{2}{V^2} \int_P^{P_0} V\,dP \Bigg|_{i=N}$$

so that upon convergence G approaches G_m.

Although the governing equations appear to be straightforward, their solution is not. We assumed a

constant flow coefficient of 0.75 to account for entrance losses with low carryover in order to expedite a solution. Fluid properties were calculated by using GASP (ref. 14).

At the 30-diameter spacing each inlet was assumed to act independently of the previous inlet. In each case it must be assumed (1) that the pressure ratio across the first inlet is known, (2) that the choking condition applies to the last inlet, and (3) that the iteration will converge to a solution.

It was difficult to apply these governing equations to flows near the critical region, but the flow above and below the critical region, $T_r < 0.9$ and $T_r > 1.1$, was apparently well described. At the last inlet ($i=N$) low pressures and those near saturation may necessitate the use of the nonequilibrium model, which allows a certain degree of metastability. This becomes important for the pressures involved. The nonequilibrium model better represents the flows in these regions, as demonstrated in references 5 and 7. The results are discussed in the next section.

At the 0.8-diameter spacing in the N-inlet configuration it was assumed that the flow was only affected by one inlet because of the jetting condition at this spacing. This assumption was based on our experimental results, which were limited to $N=4$. At some other number of inlets this assumption may no longer apply.

Results

Experimental Results

The experimental results covering a wide range of temperatures and pressures are now presented in two sections: flow rates and pressure profiles.

Flow rates.—Reduced flow rates as a function of reduced pressure at selected isotherms are presented in figure 5. The reduced flow rate was determined by

$$G_r = \frac{G}{G^*}$$

where G^* was determined by the extended corresponding-states theory (refs. 5, 15, and 16).

The flow rates for two to four sequential Borda inlets at a spacing of 30 diameters (figs. 5(a), (b), and (c)) showed very similar trends. They compared very well, having similar forms, with the limiting case of a single Borda inlet (fig. 5(d)). For $N=2$ to 4 the 0.9 reduced-temperature isotherm had a tendency to arc toward the 0.68 reduced-temperature isotherm. This characteristic "bulge" has been noted in several other experiments (e.g., refs. 15 to 19). The calculated flow rates at the 0.9 reduced-temperature isotherm did not exhibit this tendency.

The calculated flow rates for liquid and gas for two to four sequential inlets approximated the experimental curves fairly well. The calculated flow rates for the liquid ($T_r=0.68$) always were higher than the experimental flow rates. This characteristic had been previously encountered (refs. 4 and 17). The theoretical flow rates for the gas always were close to the experimental values. The calculated curve fit the four-sequential-Borda-inlet data better than did the calculated curve for the two sequential Borda inlets. The assumption of a constant flow coefficient of 0.75 was not correct even though it was used to describe the four-sequential-inlet case.

At the 0.8-diameter spacing the flow rates (figs. 5(e), (f), and (g)) again had very similar trends. These flow rates were substantially higher than those for the 30-diameter spacing but also corresponded, in form and magnitude, to those of a single inlet (fig. 5(d)).

Flow rates for selected temperatures and pressures as a function of N at the 30-diameter spacing are given in figure 6. The plotted flow rates for the experimental data were determined from the "smoothed" curves of figures 5(a) to (d). The slopes were calculated by using the least-squares technique. The slopes varied with reduced temperature and varied slightly with reduced pressure.

Pressure profile.—The variation of pressure profiles with inlet stagnation temperature is shown in figure 7. As the spacings changed from 0.8 diameter to 30 diameters, the pressure profiles changed drastically.

At the 30-diameter spacing (figs. 7(a) to (c)) the pressure profiles exhibited somewhat of a sharp drop at the entrance of the first inlet and recovered slightly within the spacer chamber. The two- and four-sequential-Borda-inlet configurations exhibited similar trends. At the lower inlet stagnation temperatures the pressure profile was flat at the last inlet. This is an indication of jetting (refs. 1 to 3, 5, 7, and 8). The pressure recovery varied the most in the last inlet.

Figure 8 provides a comparison of the pressure profiles of the last inlet of the N-sequential-Borda configuration at the 30-diameter spacing. The two- and four-sequential-inlet configurations showed very similar trends. Although the single Borda inlet (ref. 10) was not instrumented along the Borda tube, this comparison gives an idea of what was expected there. Jetting occurred at the lower inlet stagnation temperatures, but the higher inlet temperatures exhibited an arced profile.

At the 0.8-diameter spacing (figs. 7(d) to (f)) the profiles at the lower inlet stagnation temperatures resembled that of a free jet. The fluid seemed to flow almost unimpeded through the inlets, even though they were separated by 0.8 diameter. At the higher inlet stagnation temperatures the sharp drop at the first inlet was followed by a slow recovery, somewhere between that of the free jet and those of the sequential inlets spaced at 30 diameters. For $N=3$ at the 0.9 and 1.0 reduced-temperature isotherms, the pressure profile

indicated a more complete recovery. This may have some correlation with the "arc" in the flow rates at the 0.9 reduced-temperature isotherm.

Further comparisons and other data including the effects of backpressure can be found in references 1 to 3, 5, 7, and 8.

Analytic Comparisons

At the 30-diameter spacing the inlets should act independently of each other. The constant flow coefficient used to predict the flow rates caused some problems. Problems were also encountered when trying to calculate flows near the critical region.

Figure 6 presents the calculated flow rates of the N sequential Borda inlets and the experimental flow rates for the 30-diameter spacing. The flow rates seemed to follow the empirical relation

$$G_r \propto N^{-b}$$

where N denotes the number of inlets and b is weakly dependent on inlet stagnation temperature and pressure but is nominally 0.4.

With further normalizing of the reduced mass flow rate by flow through a single inlet

$$\frac{G_r}{G_{r,1}} = N^{-b}$$

For gases the $G_{r,1}$ $(T_{r,0}, P_{r,0})$ can be described by (ref. 20)

$$G_{r,1}\frac{\sqrt{T_{r,1}}}{P_{r,0}} = \frac{C_f}{5}$$

but for fluids $G_{r,1}$ $(T_{r,0}, P_{r,0})$ is more complex and the generalized flow charts of reference 21 should be used. Thus, if b is known, the mass flow rate for N well-separated[1] sequential inlets follows directly from knowing the mass flow rate for a single inlet. Furthermore, the mass flow rate is governed by the inlet stagnation conditions of the first inlet. The exponent b is given in figure 9 as a function of reduced temperature for various reduced pressures. The exponent exhibits a sine type of behavior with respect to temperature; behavior in the critical region is unknown. In the absence of information figure 9 can be used to determine $b(T_{r,0})$, or $b(T_{r,0})$ can be taken as a constant ($b \sim 0.4$).

[1] $L/D > 30$ for our geometry—in general it is cavity-geometry and Reynolds-number dependent.

The exponents for experimental flow rates below the thermodynamic critical region were greater than those for flows above that region (fig. 6). An exponent of greater magnitude indicates a lower flow rate. Hence, as the temperature increases from below critical to above critical, the flow coefficient should increase: this was illustrated in reference 5 for $N=4$.

The calculated flows had a different tendency in the exponents. The exponents for flows above the critical region were somewhat greater in magnitude than those for flows below the critical region. This difference between experiment and theory can be attributed to a directional alining effect of the Borda (ref. 8). The inlets separated by 30 diameters were assumed to act independently of each other, but there may be some carryover effects due to the alinement of the flow at the lower inlet stagnation temperatures. This would decrease the magnitude of the exponent from that calculated at the lower inlet stagnation temperatures.

Although the experimental exponents of the flow rates lay below theoretical and losses were not accounted for in the theoretical analysis, both the calculated and experimental exponents were similar in form as a function of temperature. The flow is currently an undetermined function of temperature, and figure 9 can be used as a guide.

The exponent b as a function of reduced pressure for various reduced temperatures is illustrated in figure 10; it appeared to have a weak inverse linear dependence on pressure. Again the theoretical values were higher than the experimental values. The slope appeared to decrease with an increase in pressure and would probably do so until the limiting case of an N-sequential-inlet rough tube was encountered.

Equivalent "sand" roughness will become a factor with the sequential Borda inlets spaced at 0.8 diameter. At this spacing the sequential inlets were assumed to act as a single inlet (ref. 5), but there may be a limiting value $M>N$ such that, as N approaches M, surface and equivalent roughness will become a strong factor (ref. 2).

Summary of Results

Choked flow rate and pressure profile data were taken and studied for up to four sequential Borda inlets for spacings of 30 and 0.8 diameter. At a spacing of 30 diameters the pressure profiles exhibited a sharp drop at the first inlet followed by some recovery. Fluid jetting sometimes occurred in the last inlet at the lower inlet stagnation temperatures. At a spacing of 0.8 diameter fluid jetting was prevalent throughout all of the sequential inlets at the lower inlet stagnation temperatures. The flow rates were the same as that for a single inlet.

Analytic modeling is complex, but a simplistic model of the 30-diameter spacing appeared to give good correlation with the experimental data away from the thermodynamic critical region. The data seemed to follow the simple empirical relation

$$\frac{G_r}{G_{r,1}} = N^{-b}$$

where b is a function of temperature and is weakly dependent on pressure; b is nominally 0.4. The principal feature of these results is that the mass flow rate of a single inlet can be used to readily approximate the mass flow rate of N sequential inlets. Furthermore, the mass flow rate has been shown to be governed by the stagnation conditions upstream of the first inlet and independent of downstream conditions.

National Aeronautics and Space Administration
Lewis Research Center
Cleveland, Ohio, March 7, 1984

References

1. Hendricks, R. C.: An Experimental Study of Fluid Flow Through Annuli Simulating Shaft Seals and Rotor Dynamics for the Shuttle Engine Turbopump. NASA TP-1849, 1985.
2. Hendricks, R. C.: Some Aspects of a Free Jet Phenomena to 105 *L/D* in a Constant Area Duct. Presented at 15th International Congress on Refrigeration (Venice, Italy), Sept. 23-29, 1979.
3. Hendricks, R. C.: Free Jet Phenomena in a 90° Sharp Edge Inlet Geometry. Presented at International Cryogenic Engineering Conference and International Cryogenic Materials Conference (Madison, Wis.), Aug. 21-24, 1979.
4. Hendricks, R. C.; and Poolos, N. P.: Critical Mass Flux Through Short Borda Type Inlets of Various Cross-Sections. Presented at 15th International Congress on Refrigeration (Venice, Italy), Sept. 23-29, 1979.
5. Hendricks, R. C.; and Stetz, T. T.: Some Flow Phenomena Associated with Aligned, Sequential Apertures with Borda-Type Inlets. NASA TP-1792, 1981.
6. Hendricks, R. C.; and Simoneau, R. J.: Some Flow Phenomena in a Constant Area Duct with a Borda Type Inlet Including the Critical Region. NASA TM-78943, 1978.
7. Hendricks, R. C.; and Stetz, T. T.: FLow Through Aligned Sequential Orifice Type Inlets. NASA TP-1967, 1982.
8. Hendricks, R. C.; and Stetz, T. T.: Flow Through Axially Aligned Sequential Apertures of the Orifice and Borda Types. NASA TM-81681, 1981.
9. Boscole, R. A.; Martin, J. M.; and Dennis, W. E.: An Investigation of Fluid Flow Through Orifices in Series. M.S. Thesis, M.I.T., 1949.
10. Benckert, H.; and Wachter, J.: Flow Induced Spring Coefficients of Labyrinth Seals for Application in Rotordynamics. Rotordynamic Instability Problems in High-Performance Turbomachinery. NASA CP-2133, 1980, pp. 189-212.
11. Iwatsubo, T.: Evaluation of Instability Forces of Labyrinth Seals in Turbines or Compressors. Rotordynamic Instability Problems in High-Performance Turbomachinery. NASA CP-2133, 1980, pp. 139-167.
12. Komotori, K; and Mori, H.: Leakage Characteristics of Labyrinth Seals. Proceedings of Fifth International Conference on Fluid Sealing, A. L. King, et al., eds. British Hydromechanics Research Association, 1971, pp. E4-45 through E4-63.
13. Hendricks, R. C.; et al.: Experimental Heat-Transfer Results for Cryogenic Hydrogen Flowing in Tubes at Subcritical and Supercritical Pressures to 800 Pounds per Square Inch Absolute. NASA TN D-3095, 1966.
14. Hendricks, R. C.; Baŕon, A. K.; and Peller, I. C.: GASP: A Computer Code for Calculating the Thermodynamic and Transport Properties for Ten Fluids: Parahydrogen, Helium, Neon, Methane, Nitrogen, Carbon Monoxide, Oxygen, Fluorine, Argon, and Carbon Dioxide. NASA TN D-7808, 1975.
15. Hendricks, R. C.: Normalizing Parameters for the Critical Flow Rate of Simple Fluids Through Nozzles. Proceedings of Fifth International Cryogenic Engineering Conference, K. Mendelssohn, ed., IPC Science and Technology Press, 1974, pp. 278-281.
16. Hendricks, R. C.; and Sengers, J. V.: Application of the Principle of Similarity to Fluid Mechanics. Presented at 9th International Conference on Properties of Steam (Munich, West Germany), Sept. 8-14, 1979. NASA TM-79258, 1979.
17. Simoneau, R. J.; and Hendricks, R. C.: Two-Phase Choked Flow of Cryogenic Fluids in Converging-Diverging Nozzles. NASA TP-1484, 1979.
18. Hendricks, R. C.; Simoneau, R. J.; and Barrows, R. F.: Two-Phase Choked Flow of Subcooled Oxygen and Nitrogen Through Convergent-Divergent Nozzles. NASA TN D-8169, 1976.
19. Simoneau, R. J.: Depressurization and Two-Phase Flow of Water Containing High Levels of Dissolved Nitrogen Gases. NASA TP-1839, 1981.
20. Hendricks, R. C.: Some Flow Characteristics of Conventional and Tapered High-Pressure-Drop Simulated Seals. Presented at ASME-ASLE Lubrication Conference (Dayton, Ohio), Oct. 16-18, 1979.
21. Simoneau, R. J.; and Hendricks, R. C.: Generalized Charts for Computation of Two-Phase Choked Flow of Simple Cryogenic Liquids. Cryogenics, vol. 17, no. 2, Feb. 1977, pp. 73-76.

TABLE I. - DATA FOR TWO SEQUENTIAL, AXIALLY ALINED BORDA INLETS - 30-DIAMETER SPACING

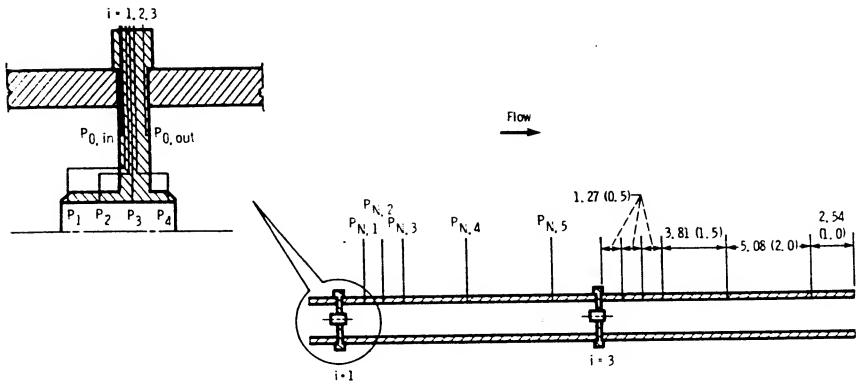

[1] RUN	MASS FLOW G/S	TIN K	PIN MPA	PBACK MPA	PR	GR	TR
ORIFICE INLET			PO,IN MPA	$P_{N,1}$ P1 MPA	$P_{N,2}$ P2 MPA	$P_{N,3}$ P3 MPA	$P_{N,4}$ P4 MPA	$P_{N,5}$ POUT MPA
3533	358.8	126.2	4.102	0.000	1.200	0.333	0.999
		1	4.11	2.89	3.21	3.42	3.44
			3.46	3.46	3.46	3.49	
		2	3.53	0.00	3.50	1.73	1.82
			1.73	0.41	0.43	1.58	0.45
			0.52	0.57	0.55	0.00	0.00
3534	264.3	126.3	3.397	0.000	0.994	0.246	1.000
		1	3.40	2.49	2.70	2.85	2.86
			2.89	2.89	2.89	2.91	
		2	2.93	0.00	2.91	1.34	1.44
			1.38	0.31	0.33	1.26	0.35
			0.40	0.44	0.42	0.00	0.00
3535	133.6	126.7	2.577	0.000	0.754	0.124	1.003
		1	2.58	1.69	1.98	2.08	2.09
			2.11	2.10	2.11	2.12	
		2	2.25	0.00	2.13	0.59	0.89
			0.89	0.19	0.21	0.85	0.21
			0.25	0.30	0.27	0.00	0.00
3536	96.3	126.4	1.963	0.000	0.574	0.089	1.001
		1	1.95	1.24	1.49	1.55	1.56
			1.57	1.57	1.58	1.58	
		2	1.62	0.00	1.60	0.33	0.61
			0.63	0.16	0.18	0.56	0.17
			0.19	0.24	0.31	0.00	0.00
			0.61	0.61	0.62	0.62	
3537	34.5	126.6	0.776	0.000	0.227	0.032	1.002
		1	0.76	0.48	0.60	0.61	0.61
		2	0.63	0.00	0.62	0.12	0.21
			0.22	0.13	0.14	0.18	0.13
			0.14	0.16	0.13	0.00	0.00
3538	403.9	141.3	6.231	0.000	1.824	0.375	1.119
		1	6.24	4.01	4.69	5.00	5.03
			5.06	5.07	5.06	5.11	
		2	5.16	0.00	5.13	1.82	2.41
			1.61	0.57	0.60	2.14	0.60
			0.70	0.82	0.80	0.00	0.00
3539	220.7	140.6	4.173	0.000	1.221	0.205	1.113
		1	4.15	2.67	2.93	3.32	3.34
			3.37	3.33	3.37	3.40	
		2	3.44	0.00	3.42	0.86	1.47
			1.44	0.29	0.31	1.38	0.33
			0.39	0.46	0.43	0.00	0.00

[1] RUN	MASS FLOW G/S	TIN K	PIN MPA	PBACK MPA	PR	GR	TR
ORIFICE INLET			PO,IN MPA	$P_{N,1}$ P1 MPA	$P_{N,2}$ P2 MPA	$P_{N,3}$ P3 MPA	$P_{N,4}$ P4 MPA	$P_{N,5}$ POUT MPA
3540	93.8	141.6	2.071	0.000	0.606	0.087	1.121
		1	2.02	1.29	1.53	1.61	1.62
			1.63	1.63	1.64	1.64	
		2	1.67	0.00	1.66	0.30	0.57
			0.59	0.17	0.18	0.49	0.17
			0.20	0.25	0.22	0.00	0.00
3541	68.2	141.2	1.547	0.000	0.453	0.063	1.118
		1	1.51	0.95	1.15	1.20	1.21
			1.22	1.22	1.22	1.22	
		2	1.24	0.00	1.24	0.23	0.42
			0.44	0.15	0.16	0.36	0.15
			0.17	0.20	0.18	0.00	0.00
3542	46.2	141.1	1.070	0.000	0.313	0.043	1.117
		1	1.04	0.65	0.80	0.82	0.83
			0.83	0.83	0.83	0.84	
		2	0.86	0.00	0.84	0.16	0.29
			0.30	0.13	0.15	0.24	0.14
			0.15	0.17	0.15	0.00	0.00
3543	599.5	127.3	6.575	0.000	1.924	0.557	1.008
		1	6.56	3.49	4.49	4.89	4.90
			4.96	4.97	4.96	5.02	
		2	5.09	0.00	5.07	1.68	2.18
			2.21	0.61	0.65	2.00	0.69
			0.78	0.86	0.84	0.00	0.00
3544	438.7	125.6	4.634	0.000	1.356	0.408	0.994
		1	4.60	2.91	3.46	35.89	3.69
			..72	3.73	3.72	3.76	
		2	3.80	0.00	3.78	1.89	2.23
			1.98	0.46	0.49	1.80	0.53
			0.60	0.65	0.65	0.00	0.00
3545	451.7	126.3	4.842	0.000	1.417	0.420	1.000
		1	4.82	3.02	3.60	3.84	3.85
			3.89	3.89	3.88	3.92	
		2	3.96	0.00	3.95	1.89	2.26
			2.01	0.47	0.50	1.84	0.54
			0.62	0.67	0.67	0.00	0.00

TABLE II. - DATA FOR TWO SEQUENTIAL, AXIALLY ALINED BORDA INLETS - 30-DIAMETER SPACING WITH APPLIED BACKPRESSURE

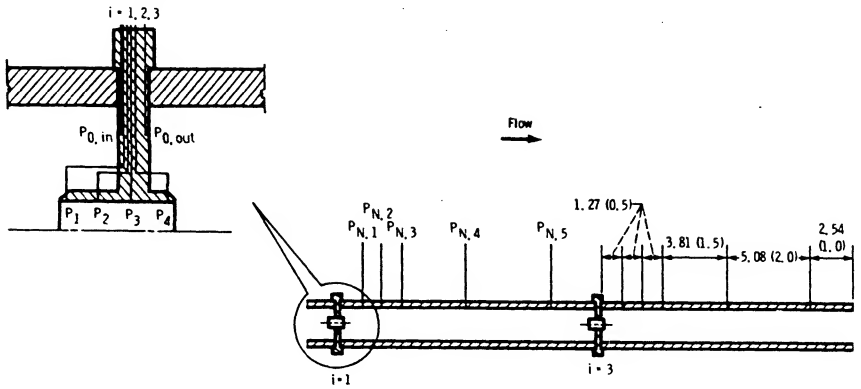

[1]

RUN	MASS FLOW G/S	TIN K	PIN MPA	PBACK MPA	PR	GR	TR
ORIFICE	INLET		POIN MPA	P1 MPA	P2 MPA	P3 MPA	P4 MPA	POUT MPA
			$P_{N,1}$	$P_{N,2}$	$P_{N,3}$	$P_{N,4}$	$P_{N,5}$	
3510	28.1	287.5	0.995	0.000	0.291	0.026	2.276	
	1		0.96	0.63	0.75	0.78	0.77	
			0.77	0.77	0.77	0.78		
	2		0.78	0.80	0.80	0.15	0.27	
			0.28	0.13	0.14	0.24	0.14	
			0.14	0.17	0.19	0.00	0.00	
3511	53.7	292.0	1.907	0.000	0.558	0.050	2.312	
	1		1.89	1.21	1.43	1.50	1.50	
			1.51	1.51	1.51	1.51		
	2		1.53	1.55	1.54	0.29	0.53	
			0.54	0.17	0.17	0.46	0.17	
			0.19	0.23	0.26	0.00	0.00	
3512	95.5	290.1	3.332	0.000	0.975	0.089	2.297	
	1		3.33	2.12	2.51	2.64	2.64	
			2.66	2.66	2.66	2.68		
	2		2.71	2.73	2.71	0.49	0.91	
			0.95	0.24	0.25	0.79	0.25	
			0.29	0.36	0.39	0.00	0.00	
3513	178.3	298.4	6.243	0.000	1.827	0.166	2.363	
	1		6.26	3.96	4.66	4.95	4.95	
			5.02	5.03	5.02	5.06		
	2		5.10	5.14	5.10	0.86	1.72	
			1.77	0.41	0.42	1.44	0.42	
			0.49	0.64	0.68	0.00	0.00	
3514	131.1	281.4	4.444	0.000	1.301	0.122	2.228	
	1		4.44	2.82	3.33	3.52	3.52	
			3.57	3.57	3.56	3.59		
	2		3.62	3.65	3.62	0.64	1.22	
			1.26	0.30	0.32	1.03	0.31	
			0.36	0.47	0.50	0.00	0.00	
3515	62.2	279.5	2.123	0.000	0.621	0.058	2.213	
	1		2.09	1.33	1.59	1.66	1.66	
			1.69	1.69	1.68	1.69		
	2		1.71	1.73	1.72	0.32	0.58	
			0.60	0.17	0.18	0.49	0.18	
			0.20	0.25	0.27	0.00	0.00	
3516	18.1	281.5	0.638	0.000	0.187	0.017	2.229	
	1		0.61	0.40	0.47	0.49	0.49	
			0.49	0.49	0.49	0.49		
	2		0.50	0.50	0.57	0.18	0.00	
			0.18	0.13	0.14	0.16	0.13	
			0.14	0.15	0.18	0.00	0.00	
3517	806.4	85.6	5.865	0.000	1.716	0.749	0.678	
	1		5.83	2.00	3.24	3.76	3.78	
			3.85	3.85	3.84	3.90		
	2		4.00	4.03	4.00	0.12	0.13	
			0.12	0.13	0.14	0.15	0.13	
			0.14	0.18	0.26	0.00	0.00	

[1]

RUN	MASS FLOW G/S	TIN K	PIN MPA	PBACK MPA	PR	GR	TR
ORIFICE	INLET		POIN MPA	P1 MPA	P2 MPA	P3 MPA	P4 MPA	POUT MPA
			$P_{N,1}$	$P_{N,2}$	$P_{N,3}$	$P_{N,4}$	$P_{N,5}$	
3518	795.0	86.8	5.875	0.000	1.719	0.739	0.687	
	1		5.84	2.07	3.30	3.80	3.82	
			3.89	3.89	3.89	3.94		
	2		4.04	4.07	4.04	0.22	0.20	
			0.22	0.73	0.76	0.38	0.74	
			0.86	0.98	0.98	0.00	0.00	
3519	691.6	87.6	4.488	0.000	1.313	0.643	0.694	
	1		4.44	1.54	2.49	2.88	2.89	
			2.95	2.94	2.94	2.98		
	2		3.06	3.09	3.06	0.13	0.13	
			0.13	0.12	0.13	0.17	0.12	
			0.13	0.18	0.24	0.00	0.00	
3520	685.3	86.7	4.489	0.000	1.314	0.637	0.686	
	1		4.45	1.62	2.53	2.92	2.93	
			2.98	2.98	2.98	3.02		
	2		3.09	3.12	3.10	0.22	0.21	
			0.23	0.63	0.65	0.36	0.63	
			0.73	0.80	0.81	0.00	0.00	
3521	572.7	84.9	3.143	0.000	0.920	0.532	0.672	
	1		3.11	1.11	1.78	2.03	2.04	
			2.08	2.07	2.08	2.10		
	2		2.15	2.18	2.16	0.15	0.15	
			0.15	0.16	0.17	0.17	0.16	
			0.16	0.18	0.24	0.00	0.00	
3522	462.2	84.5	2.120	0.000	0.620	0.430	0.669	
	1		2.09	0.79	1.22	1.38	1.39	
			1.41	1.41	1.41	1.43		
	2		1.46	1.48	1.47	0.16	0.16	
			0.16	0.17	0.18	0.17	0.17	
			0.17	0.18	0.22	0.00	0.00	
3523	347.1	85.1	1.323	0.000	0.387	0.323	0.674	
	1		1.29	0.54	0.80	0.89	0.89	
			0.91	0.90	0.91	0.93		
	2		0.94	0.94	0.94	0.18	0.19	
			0.18	0.19	0.20	0.19	0.19	
			0.20	0.20	0.23	0.00	0.00	
3524	679.5	114.2	5.731	0.000	1.677	0.632	0.904	
	1		5.71	2.37	3.43	3.89	3.89	
			3.97	3.96	3.96	4.01		
	2		4.10	4.12	4.09	0.61	0.61	
			0.66	0.59	0.61	0.80	0.59	
			0.62	0.72	0.79	0.00	0.00	
3525	677.7	114.2	5.730	0.000	1.677	0.630	0.904	
	1		5.71	2.35	3.44	3.89	3.89	
			3.96	3.96	3.96	4.01		
	2		4.10	4.12	4.09	0.62	0.62	
			0.68	0.59	0.60	0.82	0.59	
			0.62	0.72	0.78	0.00	0.00	

TABLE II. - Concluded.

[1] RUN	MASS FLOW G/S	TIN K	PIN MPA	PBACK MPA	PR	GR	TR	
ORIFICE	INLET		POIN MPA	$P_{N,1}$ P1 MPA	$P_{N,2}$ P2 MPA	$P_{N,3}$ P3 MPA	$P_{N,4}$ P4 MPA	$P_{N,5}$ POUT MPA
3526	555.5	113.0	4.117	0.000	1.205	0.516	0.895	
		1	4.09	1.82	2.51	2.85	2.86	
				2.90	2.90	2.90	2.93	
		2	2.99	3.02	3.00	0.63	0.64	
				0.67	0.53	0.54	0.75	0.53
				0.56	0.61	0.68	0.00	0.00
3527	11.3	11.6	0.539	0.000	0.158	0.011	0.092	
		1	0.44	1.29	1.38	1.71	1.81	
				1.83	1.82	1.83	1.84	
		2	1.89	1.89	1.89	0.59	0.59	
				0.60	0.44	0.45	0.62	0.44
				0.47	0.49	0.54	0.00	0.00

[1] RUN	MASS FLOW G/S	TIN K	PIN MPA	PBACK MPA	PR	GR	TR	
ORIFICE	INLET		POIN MPA	$P_{N,1}$ P1 MPA	$P_{N,2}$ P2 MPA	$P_{N,3}$ P3 MPA	$P_{N,4}$ P4 MPA	$P_{N,5}$ POUT MPA
3528	244.6	112.4	1.972	0.000	0.577	0.227	0.890	
		1	1.95	1.51	1.59	1.68	1.69	
				1.69	1.69	1.69	1.69	
		2	1.71	1.72	1.71	1.15	1.23	
				1.16	0.27	0.28	1.00	0.30
				0.34	0.35	0.35	0.00	0.00
3529	71.5	115.4	1.844	0.000	0.540	0.066	0.914	
		1	1.82	1.48	1.55	1.55	1.55	
				1.55	1.55	1.55	1.55	
		2	1.57	1.58	1.58	0.98	0.98	
				0.89	0.22	0.24	0.77	0.23
				0.26	0.28	0.30	0.00	0.00

TABLE III. - DATA FOR TWO SEQUENTIAL, AXIALLY ALINED BORDA INLETS - 0.8-DIAMETER SPACING

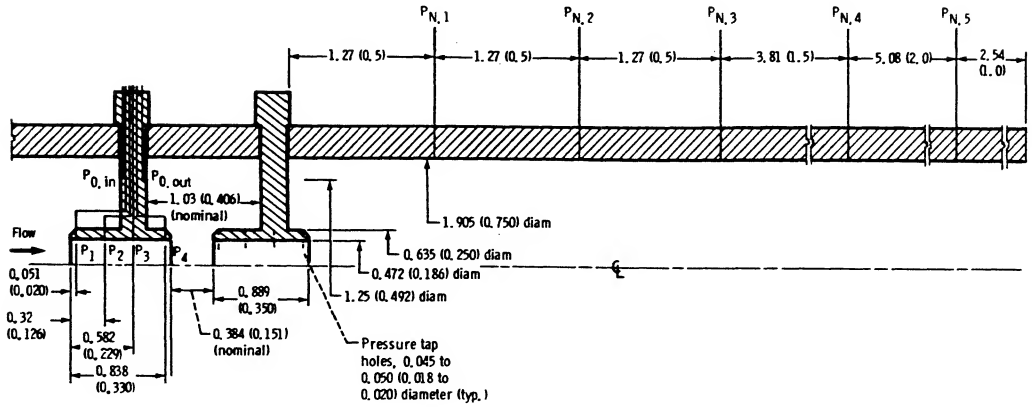

[1] XRUN	MASS FLOW G/S	TIN K	PIN MPA	PBACK MPA	PR	GR	TR
BORDA	INLET	POIN MPA	$P_{N,1}$ P1 MPA PN1	$P_{N,2}$ P2 MPA PN2	$P_{N,3}$ P3 MPA PN3	$P_{N,4}$ P4 MPA PN4	$P_{N,5}$ POUT MPA PN5
3664	42.5	255.2	1.124	0.000	0.329	0.039	2.021
	1	1.08	0.25	0.63	0.67	0.67	0.67
	2	0.68	0.52	0.54	0.50	0.43	0.14
		0.66	0.14	0.14	0.19	0.18	0.20
3665	60.4	256.9	1.585	0.000	0.464	0.056	2.034
	1	1.54	0.38	0.89	0.95	0.96	0.95
	2	0.97	0.73	0.77	0.72	0.61	0.16
		0.95	0.15	0.16	0.22	0.23	0.24
3666	95.1	261.0	2.489	0.000	0.728	0.088	2.067
	1	23.55	0.61	1.42	1.51	1.53	1.53
	2	1.53	1.11	1.20	1.12	0.98	0.22
		1.53	0.22	0.22	0.29	0.33	0.34
3667	124.4	265.1	3.266	0.000	0.956	0.116	2.099
	1	3.23	0.80	1.86	2.00	2.01	2.02
	2	2.02	1.44	1.58	1.47	1.30	0.28
		2.02	0.27	0.28	0.34	0.42	0.44
3668	155.1	269.6	4.087	0.000	1.196	0.144	2.135
	1	4.06	1.00	2.31	2.51	2.52	2.53
	2	2.53	1.79	1.97	1.84	1.64	0.34
		2.53	0.33	0.35	0.42	0.51	0.54
3669	196.6	273.6	5.194	0.000	1.520	0.183	2.166
	1	5.17	1.26	2.93	3.18	3.21	3.22
	2	3.22	2.24	2.50	2.34	2.09	0.43
		3.22	0.41	0.43	0.52	0.65	0.68
3670	835.3	84.6	4.093	0.000	1.198	0.776	0.670
	1	4.01	0.13	0.15	0.15	0.15	0.17
	2	0.17	0.17	0.18	0.17	0.18	0.11
		0.17	0.11	0.13	0.16	0.15	0.19
3671	671.9	84.7	2.763	0.000	0.809	0.624	0.671
	1	2.68	0.14	0.15	0.16	0.16	0.17
	2	0.17	0.18	0.19	0.18	0.18	0.12
		0.17	0.12	0.12	0.16	0.14	0.18
3672	536.2	84.1	1.819	0.000	0.532	0.498	0.666
	1	1.75	0.14	0.15	0.15	0.15	0.16
	2	0.17	0.17	0.18	0.17	0.17	0.12
		0.16	0.12	0.12	0.16	0.13	0.15
3673	376.9	84.2	1.012	0.000	0.296	0.350	0.667
	1	0.95	0.15	0.17	0.16	0.16	0.16
	2	0.17	0.17	0.18	0.18	0.17	0.15
		0.16	0.15	0.16	0.20	0.15	0.18

[1] XRUN	MASS FLOW G/S	TIN K	PIN MPA	PBACK MPA	PR	GR	TR
BORDA	INLET	POIN MPA	$P_{N,1}$ P1 MPA PN1	$P_{N,2}$ P2 MPA PN2	$P_{N,3}$ P3 MPA PN3	$P_{N,4}$ P4 MPA PN4	$P_{N,5}$ POUT MPA PN5
3674	641.5	116.2	3.996	0.000	1.169	0.596	0.920
	1	3.93	0.90	0.92	1.16	1.61	1.73
	2	1.75	1.70	1.71	1.69	1.57	0.59
		1.73	0.57	0.63	0.71	0.74	0.77
3675	505.1	115.8	3.098	0.000	0.907	0.469	0.917
	1	3.04	1.14	1.19	1.51	1.82	1.85
	2	1.86	1.74	1.73	1.64	1.45	0.49
		1.85	0.48	0.54	0.63	0.62	0.62
3676	371.5	114.9	2.345	0.000	0.686	0.345	0.910
	1	2.30	1.26	1.33	1.53	1.61	1.62
	2	1.62	1.46	1.42	1.31	1.14	0.39
		1.61	0.38	0.46	0.48	0.47	0.48
3677	247.2	114.5	1.856	0.000	0.543	0.230	0.907
	1	1.82	1.31	1.42	1.44	1.42	1.41
	2	1.41	1.30	1.26	1.18	1.02	0.28
		1.41	0.26	0.30	0.37	0.34	0.36
3678	481.1	139.8	5.912	0.000	1.730	0.447	1.107
	1	5.89	1.98	2.71	2.46	2.47	2.80
	2	2.80	2.82	2.89	2.83	2.65	0.59
		2.81	0.56	0.66	0.78	0.86	0.87
3679	291.8	140.8	4.351	0.000	1.273	0.271	1.115
	1	4.32	1.01	1.84	1.89	2.31	2.49
	2	2.49	2.26	2.29	2.18	1.98	0.38
		2.49	0.37	0.43	0.53	0.58	0.59
3680	114.1	139.9	1.994	0.000	0.584	0.106	1.108
	1	1.91	0.45	1.12	1.19	1.20	1.20
	2	1.20	0.90	0.95	0.89	0.79	0.19
		1.19	0.19	0.20	0.25	0.28	0.29
3681	760.8	114.9	4.903	0.000	1.435	0.707	0.910
	1	4.82	0.70	0.72	0.84	1.20	1.35
	2	1.36	1.43	1.44	1.45	1.40	0.64
		1.37	0.63	0.65	0.74	0.80	0.87
3682	568.5	114.1	3.150	0.000	0.922	0.528	0.903
	1	3.25	0.93	0.95	1.19	1.57	1.64
	2	1.66	1.59	1.60	1.55	1.40	0.52
		1.65	0.50	0.56	0.64	0.65	0.66
3683	392.0	114.3	2.400	0.000	0.702	0.364	0.905
	1	2.36	1.22	1.29	1.52	1.62	1.64
	2	1.64	1.49	1.46	1.35	1.18	0.40
		1.64	0.38	0.43	0.51	0.49	0.50

TABLE III. - Concluded.

1 XRUN	MASS FLOW G/S	TIN K	PIN MPA	PBACK MPA	PR	GR	TR					
BORDA	INLET		POIN MPA	$P_{N,1}$ P1 MPA PN1	$P_{N,2}$ P2 MPA PN2	$P_{N,3}$ P3 MPA PN3	$P_{N,4}$ P4 MPA PN4	$P_{N,5}$ P5 MPA PN5	POUT MPA			
3684	672.3	126.4	5.648	0.000	1.653	0.625	1.001					
		1	5.59	1.58	2.03	2.22	2.11	2.27				
		2	2.28	2.26	2.31	2.29	2.18	0.70				
			2.29	0.67	0.84	0.79	0.91	0.95				
3685	323.0	126.3	3.453	0.000	1.011	0.300	1.000					
		1	3.40	1.62	1.84	1.96	2.05	2.09				
		2	2.10	1.98	1.93	1.83	1.63	0.38				
			2.10	0.36	0.41	0.49	0.51	0.54				

1 RUN	MASS FLOW G/S	TIN K	PIN MPA	PBACK MPA	PR	GR	TR					
BORDA	INLET		POIN MPA	$P_{N,1}$ P1 MPA	$P_{N,2}$ P2 MPA	$P_{N,3}$ P3 MPA	$P_{N,4}$ P4 MPA	$P_{N,5}$ P5 MPA	POUT MPA			
3686	289.5	126.2	3.301	0.000	0.966	0.269	0.999					
		1	3.27	1.53	1.76	1.89	1.98	2.01				
		2	2.01	1.88	1.83	1.73	1.53	0.36				
			2.01	0.34	0.38	0.46	0.48	0.51				
3687	81.5	126.8	1.391	0.000	0.407	0.076	1.004					
		1	1.35	0.31	0.80	0.84	0.85	0.84				
		2	0.84	0.64	0.68	0.63	0.56	0.16				
			0.84	0.16	0.16	0.21	0.21	0.23				

TABLE IV. - DATA FOR THREE SEQUENTIAL, AXIALLY ALINED BORDA INLETS - 30-DIAMETER SPACING WITH APPLIED BACKPRESSURE[1]

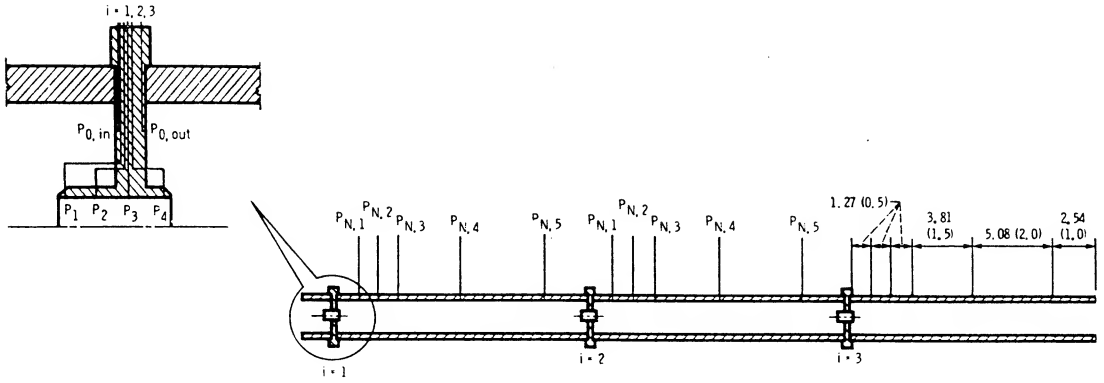

RUN	MASS FLOW G/S	TIN K	PIN MPA	PBACK MPA	PR	GR	TR					
BORDA	INLET		POIN $P_{N,1}$ MPA	P1 $P_{N,2}$ MPA	P2 $P_{N,3}$ MPA	P3 $P_{N,4}$ MPA	P4 $P_{N,5}$ MPA	POUT MPA				
3606	26.5	281.9	1.073	0.000	0.314	0.025	2.232					
	1		1.05	0.77	0.85	0.89	0.88	0.85				
				0.73	0.73	0.74	0.75	0.75				
	2		0.91	0.58	0.69	0.72	0.73	0.73				
	3		0.75	0.13	0.26	0.26	0.22	0.18				
				0.93								
3607	60.8	280.6	2.422	0.000	0.709	0.057	2.222					
	1		2.40	1.76	1.97	2.04	2.06	2.03				
				1.67	1.67	1.69	1.71	1.72				
	2		2.09	1.33	1.58	1.66	1.66	1.67				
	3		16.17	0.31	0.58	0.60	0.49	0.22				
				2.11								
3608	102.9	281.6	4.079	0.000	1.194	0.096	2.230					
	1		4.08	2.98	3.32	3.47	3.53	3.49				
				2.84	2.83	2.86	2.89	2.91				
	2		3.54	2.24	2.64	2.80	2.81	2.84				
	3		2.89	0.51	0.98	1.01	0.82	0.29				
				3.57								
3609	145.0	282.3	5.714	0.000	1.672	0.135	2.235					
	1		5.72	4.15	4.66	4.87	4.98	4.91				
				3.98	3.98	4.01	4.05	4.08				
	2		4.98	3.14	3.69	3.92	3.93	3.98				
	3		4.04	0.70	1.36	1.41	1.15	0.37				
				5.00								
3610	21.9	261.4	0.864	0.000	0.253	0.020	2.070					
	1		0.84	0.61	0.60	0.71	0.70	0.66				
				0.59	0.60	0.59	0.61	0.61				
	2		0.74	0.47	0.57	0.59	0.59	0.59				
	3		0.60	0.10	0.21	0.22	0.17	0.18				
				0.75								
3612	673.1	85.8	5.370	0.000	1.572	0.626	0.679					
	1		5.33	2.58	3.49	3.91	3.99	3.93				
				2.67	2.67	2.72	2.80	2.80				
	2		4.06	1.44	2.24	2.61	2.63	2.68				
	3		2.79	0.13	0.14	0.14	0.16	0.19				
				4.07								
3613	573.4	86.3	4.002	0.000	1.171	0.533	0.683					
	1		3.98	1.95	2.61	2.91	2.97	2.93				
				2.00	2.01	2.04	2.09	2.10				
	2		3.02	1.09	1.70	1.96	1.98	2.01				
	3		2.09	0.14	0.14	0.14	0.16	0.19				
				3.04								
3614	463.6	85.8	2.687	0.000	0.786	0.431	0.679					
	1		2.66	1.32	1.77	1.96	1.99	2.01				
				1.36	1.38	1.39	1.43	1.43				
	2		2.04	0.78	1.17	1.34	1.35	1.37				
	3		1.42	0.15	0.15	0.16	0.17	0.20				
				2.05								

RUN	MASS FLOW G/S	TIN K	PIN MPA	PBACK MPA	PR	GR	TR					
BORDA	INLET		POIN $P_{N,1}$ MPA	P1 $P_{N,2}$ MPA	P2 $P_{N,3}$ MPA	P3 $P_{N,4}$ MPA	P4 $P_{N,5}$ MPA	POUT MPA				
3615	346.9	85.9	1.623	0.000	0.475	0.322	0.680					
	1		1.60	0.84	1.08	1.19	1.20	1.21				
				0.86	0.86	0.87	0.90	0.90				
	2		1.24	0.52	0.76	0.84	0.85	0.86				
	3		0.89	0.17	0.17	0.17	0.18	0.22				
				1.26								
3616	294.8	86.2	1.246	0.000	0.365	0.274	0.683					
	1		1.22	0.67	0.84	0.92	0.92	0.88				
				0.68	0.68	0.69	0.71	0.71				
	2		0.95	0.44	0.61	0.67	0.67	0.68				
	3		0.70	0.17	0.18	0.18	0.18	0.22				
				0.98								
3617	570.1	115.2	5.487	0.000	1.606	0.530	0.912					
	1		5.45	3.01	3.78	4.15	4.24	4.19				
				3.03	3.03	3.07	3.13	3.15				
	2		4.30	1.89	2.58	2.96	2.98	3.02				
	3		3.12	0.63	0.64	0.70	0.78	0.59				
				4.32								
3618	468.8	114.5	3.957	0.000	1.158	0.436	0.907					
	1		3.93	2.22	2.78	3.03	3.09	3.03				
				2.24	2.23	2.27	2.32	2.33				
	2		3.13	1.51	1.69	2.17	2.22	2.24				
	3		2.32	0.61	0.62	0.67	0.71	0.53				
				3.15								
3619	371.9	113.5	2.814	0.000	0.824	0.346	0.899					
	1		2.80	1.71	2.04	2.22	2.24	2.20				
				1.67	1.66	1.70	1.73	1.74				
	2		2.28	1.26	1.32	1.55	1.65	1.67				
	3		1.73	0.64	0.65	0.68	0.65	0.46				
				2.30								
3620	205.1	113.8	1.935	0.000	0.566	0.191	0.901					
	1		1.92	1.58	1.66	1.72	1.73	1.69				
				1.53	1.53	1.54	1.55	1.56				
	2		1.75	1.43	1.50	1.53	1.53	1.53				
	3		1.55	1.03	1.07	0.98	0.84	0.27				
				1.77								
3622	434.5	127.3	5.355	0.000	1.567	0.404	1.008					
	1		5.53	3.81	4.35	4.61	4.70	4.66				
				3.82	3.81	3.85	3.89	3.91				
	2		4.71	3.02	3.52	3.77	3.78	3.81				
	3		3.87	1.90	2.24	1.98	1.80	0.55				
				4.74								
3623	269.0	126.8	3.729	0.000	1.091	0.250	1.004					
	1		3.73	2.96	3.15	3.30	3.35	3.30				
				2.86	2.86	2.87	2.90	2.91				
	2		3.35	2.47	2.69	2.82	2.84	2.86				
	3		2.89	1.35	1.45	1.38	1.26	0.37				
				3.38								

TABLE IV. - Concluded.

[1] RUN	MASS FLOW G/S	TIN K	PIN MPA	PBACK MPA	PR	GR	TR					
BORDA	INLET		POIN	$P_{N,1}$ P1	$P_{N,2}$ P2	$P_{N,3}$ P3	$P_{N,4}$ P4	$P_{N,5}$	POUT			
			MPA	MPA	MPA	MPA	MPA	MPA	MPA			
3624	166.8	126.3	3.301	0.000	0.966	0.155	1.000					
	1		3.30	2.55	2.75	2.87	2.92	2.87				
				2.41	2.42	2.42	2.46	2.46				
	2		2.93	2.04	2.25	2.38	2.39	2.41				
	3		2.45	0.88	1.04	1.05	0.98	0.30				
				2.95								
3625	121.7	126.8	2.681	0.000	0.785	0.113	1.004					
	1		2.67	1.99	2.20	2.29	2.32	2.33				
				1.91	1.91	1.93	1.95	1.95				
	2		2.34	1.55	1.80	1.89	1.89	1.91				
	3		1.94	0.56	0.79	0.80	0.78	0.24				
				2.35								
3626	63.7	125.9	1.545	0.000	0.452	0.059	0.997					
	1		1.53	1.11	1.24	1.29	1.30	1.26				
				1.06	1.06	1.07	1.09	1.09				
	2		1.32	0.84	1.01	1.05	1.05	1.06				
	3		1.08	0.20	0.37	0.39	0.33	0.19				
				1.35								
3627	60.8	126.8	1.496	0.000	0.438	0.057	1.004					
	1		1.48	1.07	1.20	1.25	1.26	1.23				
				1.03	1.04	1.04	1.06	1.06				
	2		1.29	0.82	0.98	1.02	1.02	1.04				
	3		1.05	0.20	0.36	0.38	0.31	0.19				
				1.30								
3628	332.5	140.2	5.987	0.000	1.752	0.309	1.110					
	1		5.98	4.43	4.89	5.13	5.23	5.18				
				4.33	4.33	4.37	4.40	4.43				
	2		5.24	3.55	4.04	4.28	4.29	4.33				
	3		4.39	1.62	1.92	1.93	1.84	0.52				
				5.26								
3629	169.0	140.4	3.667	0.000	1.073	0.149	1.112					
	1		3.66	2.69	2.98	3.11	3.17	3.11				
				2.56	2.56	2.58	2.61	2.62				
	2		3.18	2.03	2.39	2.52	2.53	2.56				
	3		2.60	0.58	1.07	1.08	0.99	0.28				
				3.21								

[1] RUN	MASS FLOW G/S	TIN K	PIN MPA	PBACK MPA	PR	GR	TR					
BORDA	INLET		POIN	$P_{N,1}$ P1	$P_{N,2}$ P2	$P_{N,3}$ P3	$P_{N,4}$ P4	$P_{N,5}$	POUT			
			MPA	MPA	MPA	MPA	MPA	MPA	MPA			
3630	89.0	140.7	2.270	0.000	0.664	0.083	1.114					
	1		2.26	1.64	1.84	1.91	1.93	1.89				
				1.57	1.57	1.58	1.60	1.61				
	2		1.96	1.24	1.47	1.55	1.55	1.57				
	3		1.60	0.29	0.55	0.57	0.48	0.21				
				1.98								
3631	688.8	87.7	5.760	0.000	1.686	0.640	0.694					
	1		5.72	2.79	3.75	4.20	4.29	4.23				
				2.88	2.87	2.92	2.99	3.02				
	2		4.35	1.55	2.41	2.80	2.82	2.88				
	3		3.00	0.15	0.15	0.16	0.20	0.21				
				4.38								
3632	524.3	88.1	3.479	0.000	1.018	0.487	0.698					
	1		3.44	1.71	2.27	2.53	2.58	2.55				
				1.76	1.75	1.79	1.83	1.84				
	2		2.63	0.98	1.50	1.72	1.73	1.76				
	3		1.83	0.17	0.17	0.18	0.19	0.22				
				2.65								
3633	358.1	87.1	1.744	0.000	0.510	0.333	0.690					
	1		1.71	0.90	1.16	1.28	1.29	1.24				
				0.91	0.91	0.93	0.95	0.95				
	2		1.33	0.55	0.81	0.90	0.90	0.92				
	3		0.95	0.18	0.18	0.22	0.18	0.22				
				1.34								
3634	511.6	90.6	3.472	0.000	1.016	0.475	0.717					
	1		3.44	1.77	2.31	2.57	2.61	2.56				
				1.82	1.82	1.85	1.89	1.90				
	2		2.66	1.08	1.57	1.79	1.79	1.82				
	3		1.89	0.29	0.29	0.31	0.14	0.73				
				2.68								
3635	515.4	91.5	3.467	0.000	1.015	0.479	0.724					
	1		3.44	1.73	2.29	2.54	2.60	2.54				
				1.78	1.78	1.81	1.84	1.86				
	2		2.64	1.01	1.52	1.74	1.75	1.78				
	3		1.85	0.21	0.22	0.22	0.31	0.27				
				2.66								

TABLE V. - DATA FOR THREE SEQUENTIAL, AXIALLY ALINED BORDA INLETS - 0.8-DIAMETER SPACING

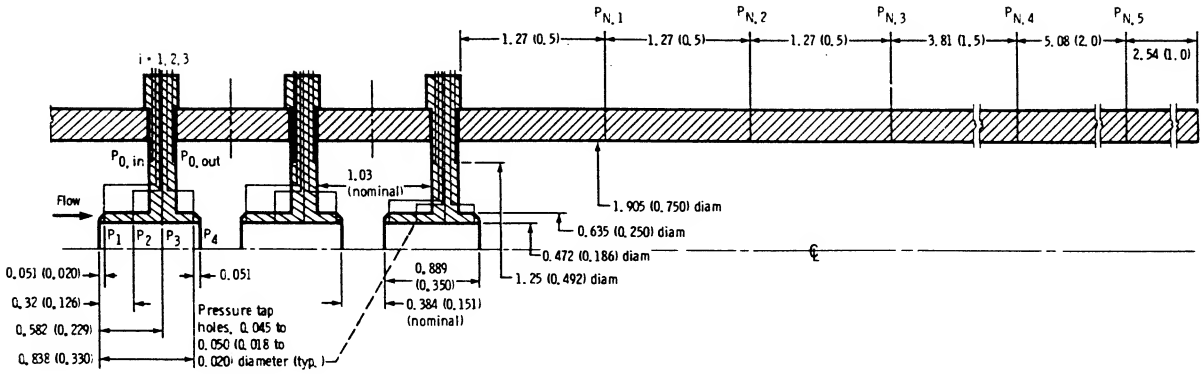

[1]

RUN	MASS FLOW G/S	TIN K	PIN MPA	PBACK MPA	PR	GR	TR

BORDA	INLET	POIN MPA	$P_{N,1}$ P1 MPA	$P_{N,2}$ P2 MPA	$P_{N,3}$ P3 MPA	$P_{N,4}$ P4 MPA	$P_{N,5}$ POUT MPA
3637	32.9	260.3	0.921	0.000	0.270	0.031	2.061
	1	0.88	0.29	0.51	0.57	0.57	0.57
			0.57				
	2	0.57	0.52	0.52	0.52	0.52	0.52
			0.52				
	3	0.51	0.40	0.44	0.38	0.36	0.14
			0.13	0.11	0.00	0.18	
3638	52.3	261.4	1.441	0.000	0.422	0.049	2.070
	1	1.40	0.47	0.80	0.91	0.91	0.91
			0.91				
	2	0.91	0.84	0.82	0.84	0.83	0.83
			0.83				
	3	0.82	0.63	0.69	0.61	0.56	0.16
			0.15	0.13	0.12	0.22	
3639	100.1	264.9	2.734	0.000	0.800	0.093	2.097
	1	2.69	0.91	1.51	1.73	1.75	1.74
			1.74				
	2	1.74	1.61	1.59	1.62	1.60	1.60
			1.60				
	3	1.60	1.19	1.30	1.17	1.05	0.24
			0.23	0.20	0.23	0.37	
3640	148.5	269.2	4.065	0.000	1.190	0.138	2.131
	1	4.04	1.34	2.24	2.58	2.62	2.60
			2.60				
	2	2.60	2.40	2.37	2.42	2.39	2.40
			2.40				
	3	2.39	1.76	1.91	1.74	1.55	0.34
			0.33	0.38	0.35	0.52	
3641	201.7	272.9	5.522	0.000	1.616	0.187	2.161
	1	5.51	1.81	3.02	3.49	3.55	3.53
			3.53				
	2	3.53	3.25	3.22	3.29	3.26	3.26
			3.26				
	3	3.26	2.36	2.56	2.36	2.10	0.44
			0.43	0.41	0.48	0.70	
3642	104.4	266.2	2.837	0.000	0.830	0.097	2.108
	1	2.80	0.95	1.58	1.80	1.82	1.81
			1.81				
	2	1.81	1.66	1.65	1.69	1.66	1.66
			1.67				
	3	1.66	1.22	1.33	1.21	1.09	0.25
			0.24	0.21	0.24	0.38	
3643	65.6	265.8	1.808	0.000	0.529	0.061	2.105
	1	1.77	0.61	1.00	1.14	1.15	1.15
			1.15				
	2	1.15	1.05	1.04	1.06	1.05	1.05
			1.06				
	3	1.05	0.78	0.85	0.77	0.70	0.18
			0.17	0.16	0.15	0.26	
3644	811.9	84.8	3.967	0.000	1.161	0.755	0.671
	1	3.89	0.13	0.15	0.15	0.15	0.17
			0.17				
	2	0.17	0.17	0.18	0.19	0.18	0.19
			0.20				
	3	0.19	0.20	0.24	0.19	0.20	0.14
			0.14	0.12	0.11	0.19	

[1]

RUN	MASS FLOW G/S	TIN K	PIN MPA	PBACK MPA	PR	GR	TR

BORDA	INLET	POIN MPA	$P_{N,1}$ P1 MPA	$P_{N,2}$ P2 MPA	$P_{N,3}$ P3 MPA	$P_{N,4}$ P4 MPA	$P_{N,5}$ POUT MPA
3645	670.9	85.1	2.799	0.000	0.819	0.624	0.674
	1	2.73	0.14	0.16	0.16	0.16	0.17
			0.17				
	2	0.17	0.17	0.18	0.19	0.18	0.20
			0.20				
	3	0.19	0.20	0.24	0.20	0.21	0.14
			0.14	0.11	0.11	0.17	
3646	567.7	84.4	2.052	0.000	0.601	0.528	0.668
	1	1.98	0.14	0.15	0.16	0.16	0.16
			0.17				
	2	0.17	0.16	0.17	0.18	0.18	0.19
			0.19				
	3	0.18	0.19	0.22	0.19	0.20	0.13
			0.13	0.11	0.00	0.16	
3647	455.0	84.5	1.401	0.000	0.410	0.423	0.669
	1	1.34	0.15	0.17	0.16	0.16	0.17
			0.17				
	2	0.17	0.17	0.18	0.19	0.18	0.19
			0.20				
	3	0.19	0.20	0.24	0.20	0.20	0.14
			0.14	0.11	0.10	0.16	
3648	379.0	84.8	1.047	0.000	0.306	0.352	0.671
	1	0.99	0.15	0.17	0.17	0.17	0.17
			0.17				
	2	0.18	0.17	0.18	0.19	0.19	0.20
			0.21				
	3	0.20	0.21	0.24	0.20	0.21	0.16
			0.16	0.17	0.12	0.18	
3649	727.1	114.7	4.644	0.000	1.359	0.676	0.908
	1	4.57	0.71	0.74	0.84	1.18	1.36
			1.36				
	2	1.36	1.40	1.40	1.45	1.46	1.64
			1.64				
	3	1.64	1.60	1.66	1.59	1.53	0.65
			0.63	0.64	0.72	0.85	
3650	573.2	114.1	3.376	0.000	0.988	0.533	0.903
	1	3.32	0.90	0.93	1.10	1.49	1.59
			1.58				
	2	1.59	1.61	1.58	1.73	1.80	1.82
			1.82				
	3	1.81	1.58	1.70	1.59	1.45	0.54
			0.52	0.56	0.63	0.70	
3651	404.8	113.5	2.473	0.000	0.724	0.376	0.899
	1	2.43	1.20	1.26	1.53	1.68	1.69
			1.69				
	2	1.69	1.64	1.64	1.66	1.65	1.66
			1.66				
	3	1.65	1.54	1.55	1.42	1.26	0.42
			0.40	0.44	0.44	0.52	
3652	207.8	113.7	1.774	0.000	0.519	0.193	0.900
	1	1.74	1.26	1.36	1.33	1.30	1.29
			1.29				
	2	1.29	1.23	1.21	1.19	1.15	1.15
			1.16				
	3	1.15	1.09	1.07	0.96	0.86	0.25
			0.23	0.21	0.24	0.32	

TABLE V. - Concluded.

[1] RUN	MASS FLOW G/S	TIN	PIN	PBACK	PR	GR	TR					
		K	MPA	MPA								
BORDA	INLET		POIN $P_{N,1}$ MPA	P1 $P_{N,2}$ MPA	P2 $P_{N,3}$ MPA	P3 $P_{N,4}$ MPA	P4 $P_{N,5}$ MPA	POUT MPA				
3653	641.4	127.0	5.560	0.000	1.627	0.596	1.006					
	1		5.51	1.66	2.05	2.30	2.16	2.30				
			2.31									
	2		2.30	2.33	2.28	2.33	2.40	2.55				
			2.56									
	3		2.55	2.52	2.54	2.46	2.32	0.71				
				0.67	0.72	0.75	0.94					
3654	247.7	126.4	3.323	0.000	0.972	0.230	1.001					
	1		3.31	1.51	1.93	2.15	2.20	2.20				
			2.20									
	2		2.20	2.09	2.06	2.08	2.06	2.07				
			2.07									
	3		2.05	1.86	1.82	1.64	1.48	0.34				
				0.33	0.31	0.37	0.49					
3655	164.7	127.5	2.644	0.000	0.774	0.153	1.010					
	1		2.62	1.03	1.62	1.78	1.80	1.78				
			1.78									
	2		1.78	1.65	1.64	1.66	1.65	1.65				
			1.64									
	3		1.63	1.33	1.40	1.25	1.13	0.24				
				0.23	0.21	0.25	0.37					
3656	127.8	126.4	2.130	0.000	0.623	0.119	1.001					
	1		2.09	0.72	1.20	1.35	1.37	1.36				
			1.35									
	2		1.36	1.25	1.24	1.26	1.25	1.24				
			1.24									
	3		1.24	0.95	1.02	0.92	0.84	0.21				
				0.20	0.28	0.20	0.31					
3657	644.3	126.8	5.555	0.000	1.626	0.599	1.004					
	1		5.50	1.64	2.03	2.29	2.16	2.29				
			2.30									
	2		2.29	2.32	2.27	2.33	2.38	2.54				
			2.55									
	3		2.54	2.51	2.55	2.45	2.31	0.71				
				0.68	0.73	0.76	0.95					

[1] RUN	MASS FLOW G/S	TIN	PIN	PBACK	PR	GR	TR					
		K	MPA	MPA								
BORDA	INLET		POIN $P_{N,1}$ MPA	P1 $P_{N,2}$ MPA	P2 $P_{N,3}$ MPA	P3 $P_{N,4}$ MPA	P4 $P_{N,5}$ MPA	POUT MPA				
3658	262.7	126.0	3.271	0.000	0.957	0.244	0.998					
	1		3.24	1.57	1.92	2.13	2.18	2.18				
			2.18									
	2		2.18	2.08	2.06	2.06	2.04	2.06				
			2.06									
	3		2.05	1.87	1.82	1.66	1.49	0.35				
				0.33	0.32	0.37	0.49					
3659	268.6	126.2	3.310	0.000	0.969	0.250	0.999					
	1		3.27	1.58	1.94	2.15	2.21	2.20				
			2.21									
	2		2.21	2.11	2.09	2.09	2.06	2.08				
			2.09									
	3		2.08	1.89	1.84	1.68	1.51	0.35				
				0.33	0.32	0.40	0.50					
3660	440.6	140.4	5.732	0.000	1.677	0.409	1.112					
	1		5.71	1.95	3.47	3.91	3.93	3.90				
			3.90									
	2		3.89	3.66	3.67	3.72	3.71	3.70				
			3.69									
	3		3.69	3.17	3.33	3.20	2.95	0.57				
				0.54	0.57	0.68	0.84					
3661	262.3	140.5	4.142	0.000	1.212	0.244	1.112					
	1		4.11	1.43	2.39	2.70	2.73	2.71				
			2.70									
	2		2.71	2.46	2.47	2.51	2.50	2.49				
			2.49									
	3		2.49	1.99	2.11	1.95	1.79	0.35				
				0.34	0.34	0.42	0.56					
3662	162.2	140.7	2.482	0.000	0.726	0.151	1.114					
	1		2.45	0.85	1.40	1.58	1.60	1.59				
			1.59									
	2		1.60	1.46	1.44	1.47	1.46	1.45				
			1.44									
	3		1.44	1.11	1.19	1.06	0.98	0.23				
				0.22	0.20	0.23	0.35					

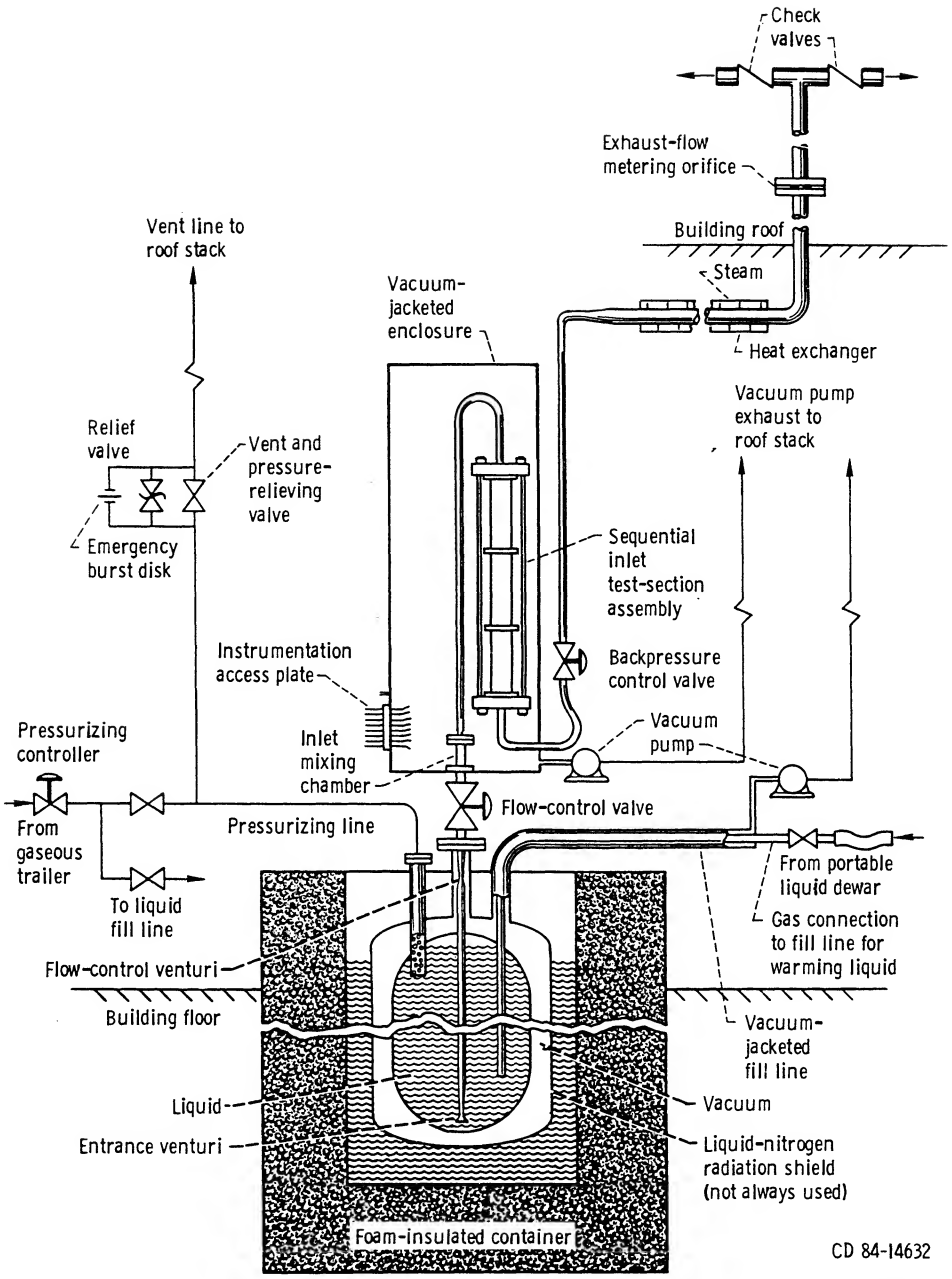

Figure 1.—Schematic diagram of high-pressure liquid flow apparatus with sequential Borda inlet configuration.

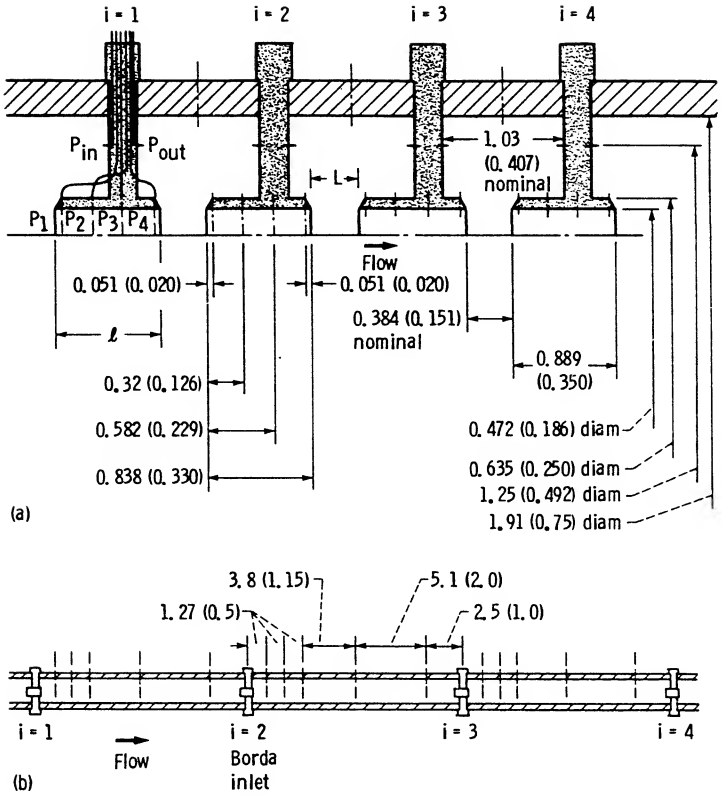

(a) 1.03-cm (0.407-in.) spacer.
(b) 15.2-cm (6.0-in.) spacer.

Figure 2.—Schematic of *N*-sequential-Borda-inlet test section. (Dimensions are in centimeter (inches).)

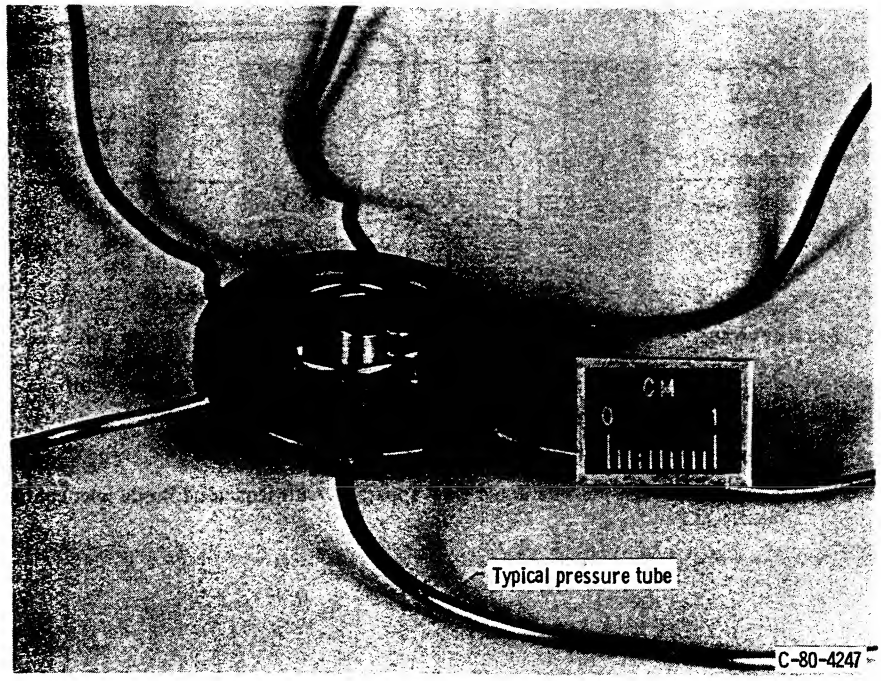

Figure 3.—Borda inlet.

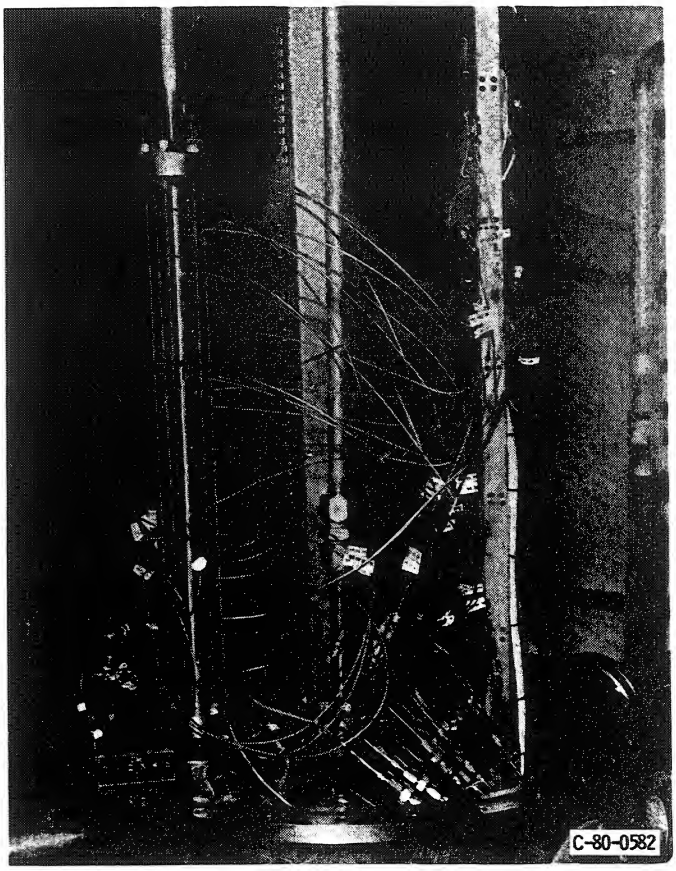

Figure 4.—Installation of three-sequential-inlet test section with 15.2-cm (6.0-in.) spacer.

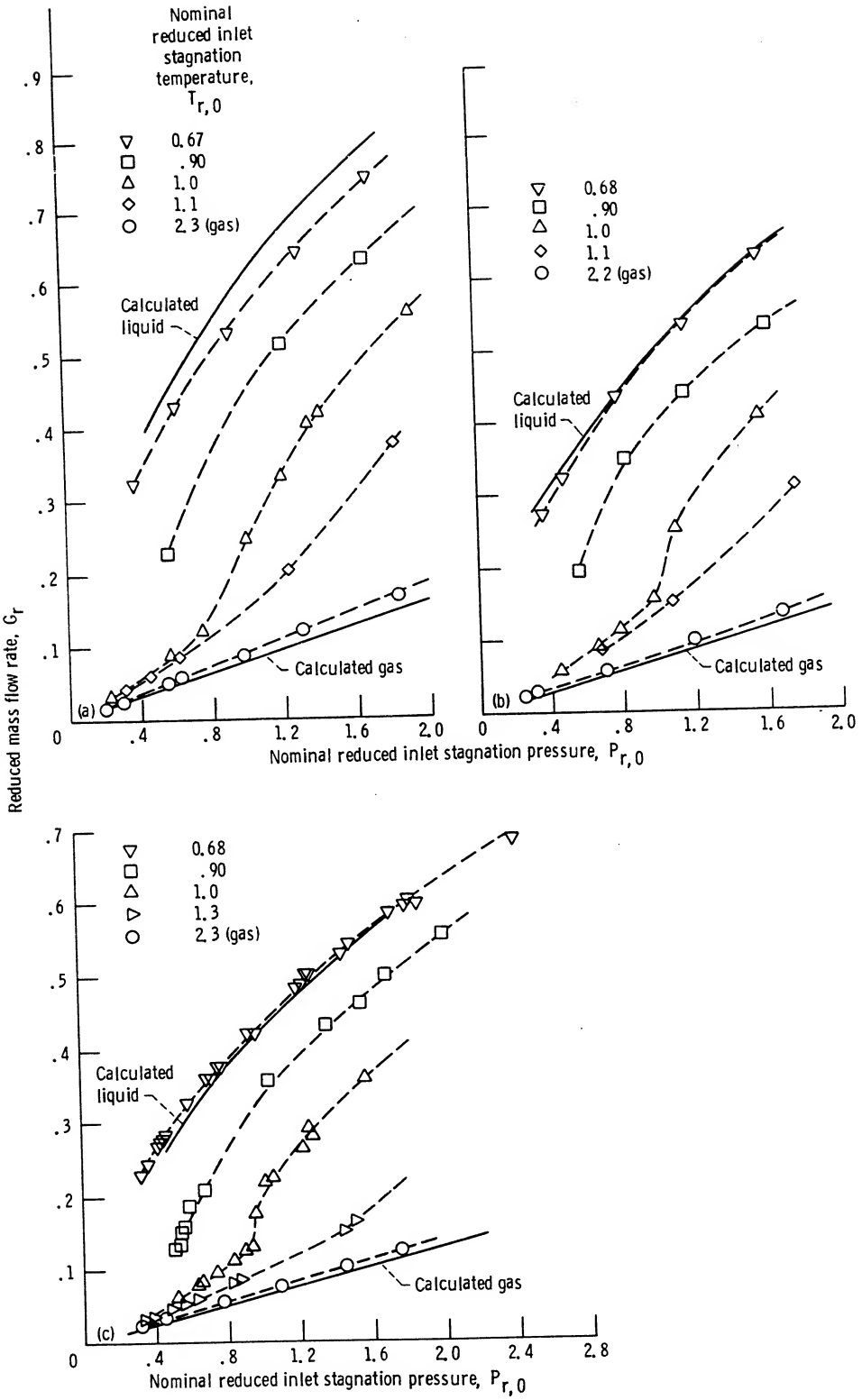

(a) Two Borda inlets at 15.2-cm (6.0-in.) spacing.
(b) Three Borda inlets at 15.2-cm (6.0-in.) spacing.
(c) Four Borda inlets at 15.2-cm (6.0-in.) spacing.

Figure 5.—Reduced mass flow rate as a function of reduced inlet stagnation pressure for selected reduced inlet stagnation temperatures.

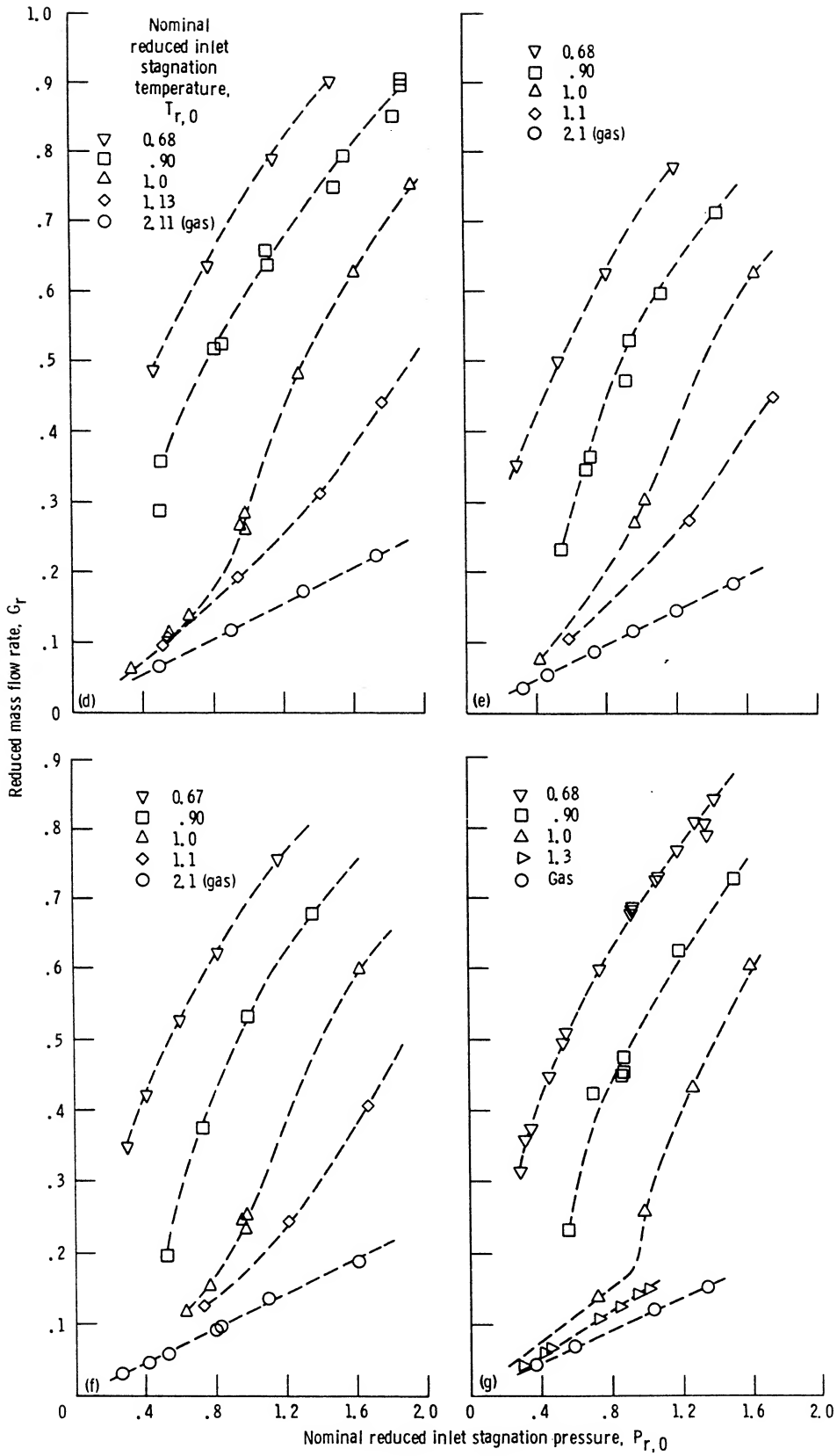

(d) Single Borda inlet.
(e) Two Borda inlets at 1.03-cm (0.407-in.) spacing.
(f) Three Borda inlets at 1.03-cm (0.407-in.) spacing.
(g) Four Borda inlets at 1.03-cm (0.407-in.) spacing.

Figure 5.—Concluded.

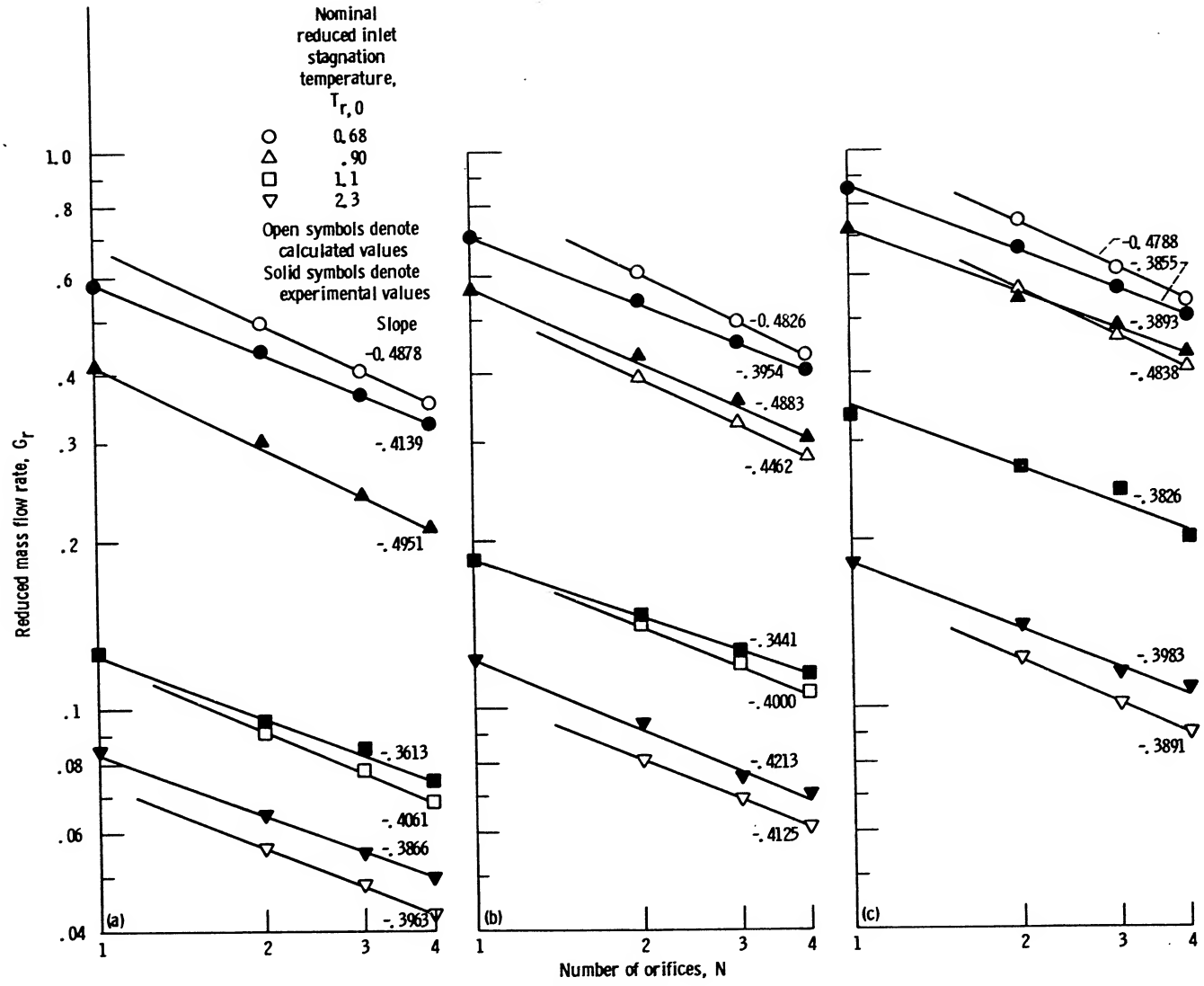

(a) $P_{r,0}$, 0.7.
(b) $P_{r,0}$, 1.0.
(c) $P_{r,0}$, 1.5.

Figure 6.—Reduced mass flow rate as a function of number of inlets for selected reduced inlet stagnation temperatures.

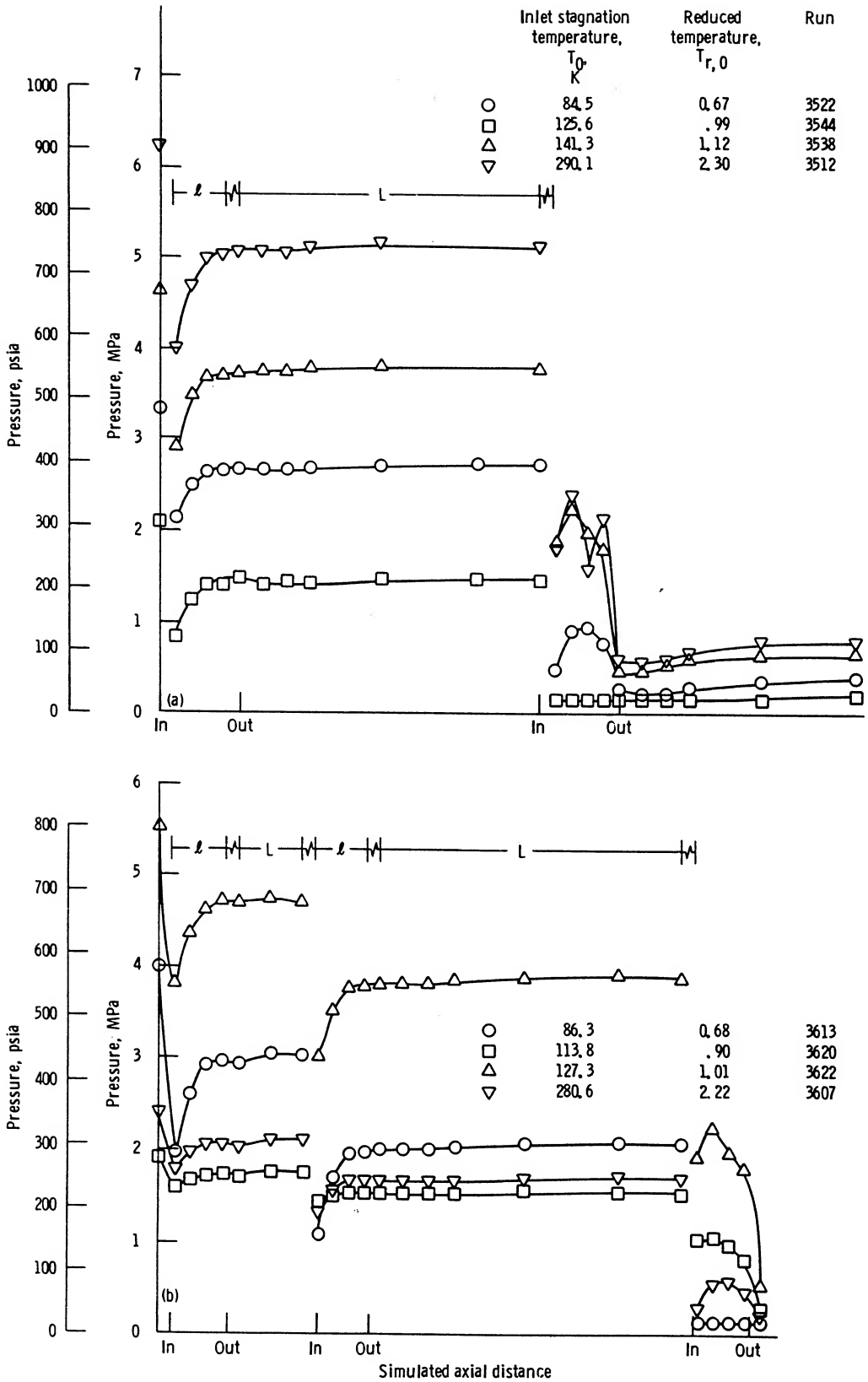

(a) Two Borda inlets at 15.2-cm (6.0-in.) spacing.
(b) Three Borda inlets at 15.2-cm (6.0-in.) spacing.

Figure 7.—Pressure profiles at selected stagnation temperatures.

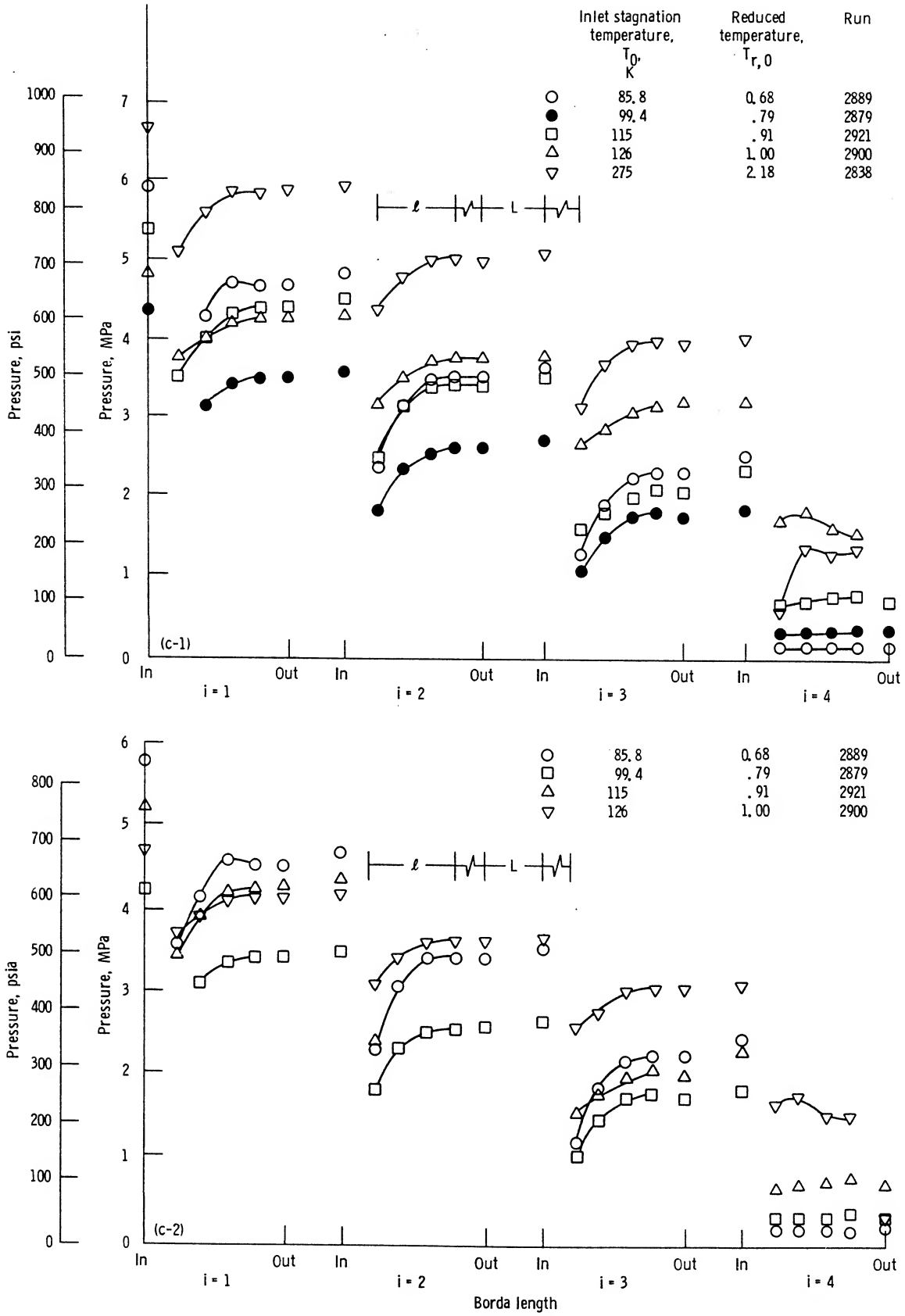

(c) Four Borda inlets at 15.2-cm (6.0-in.) spacing.

Figure 7.—Continued.

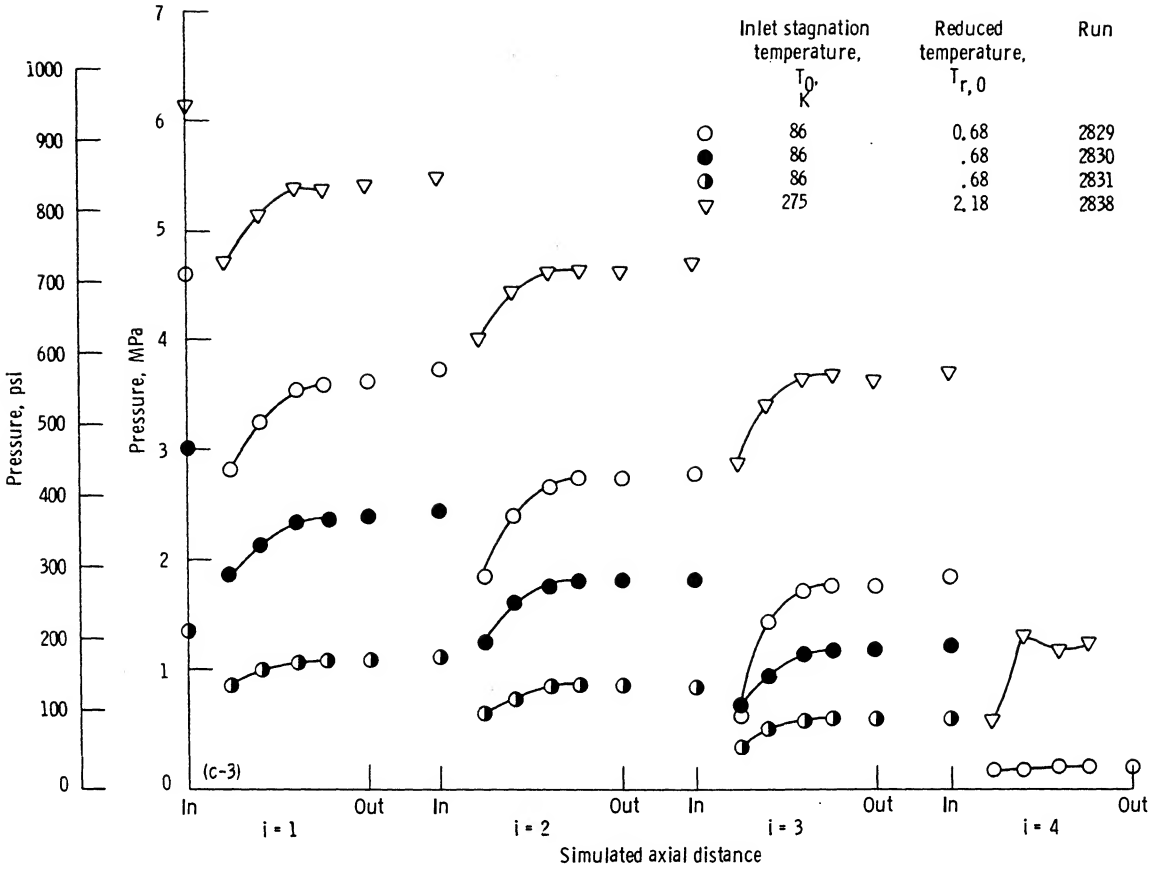

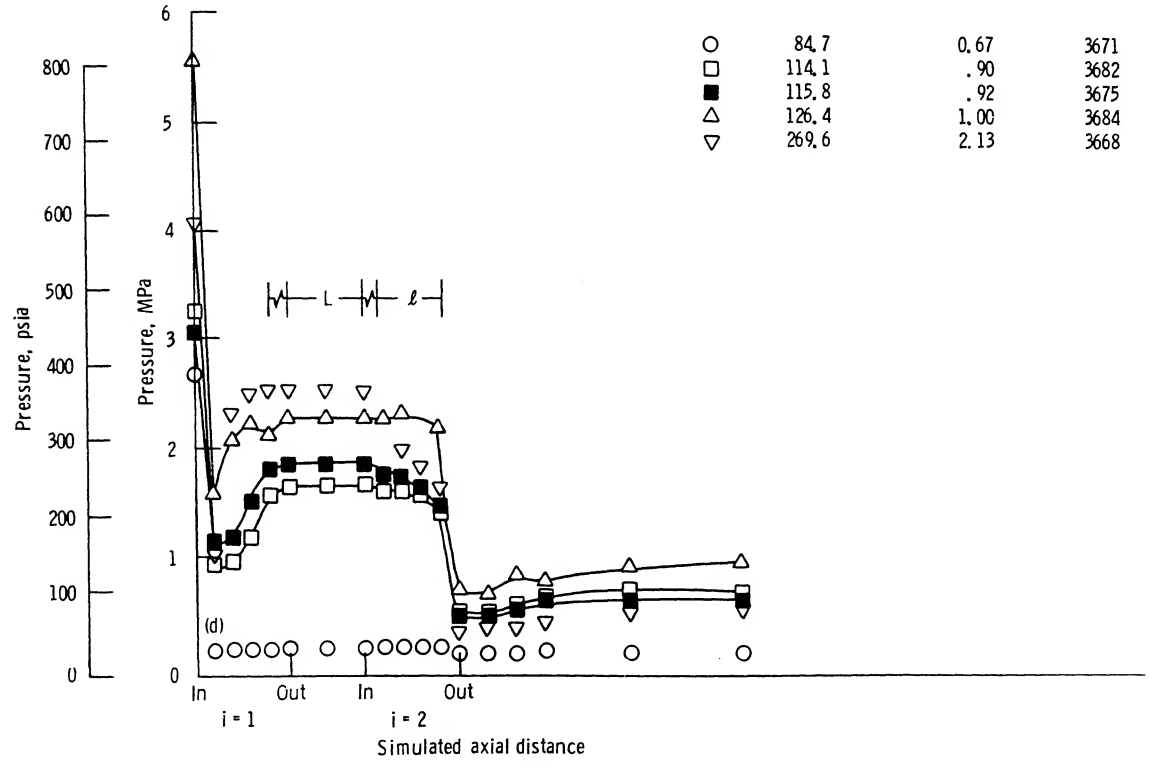

(c) Concluded.
(d) Two Borda inlets at 1.03-cm (0.407-in.) spacing.

Figure 7.—Continued.

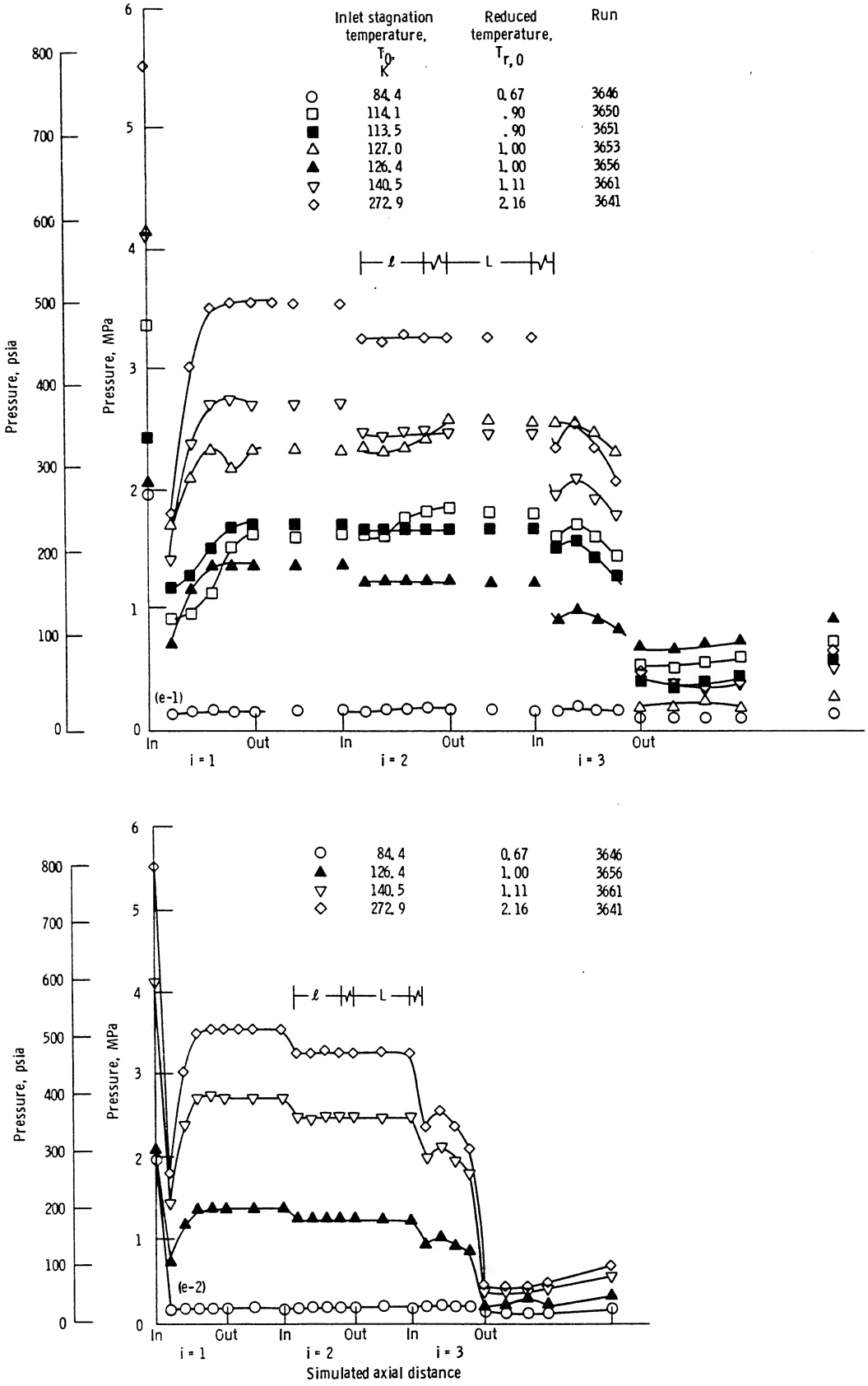

(e) Three Borda inlets at 1.03-cm (0.407-in.) spacing.

Figure 7.—Continued.

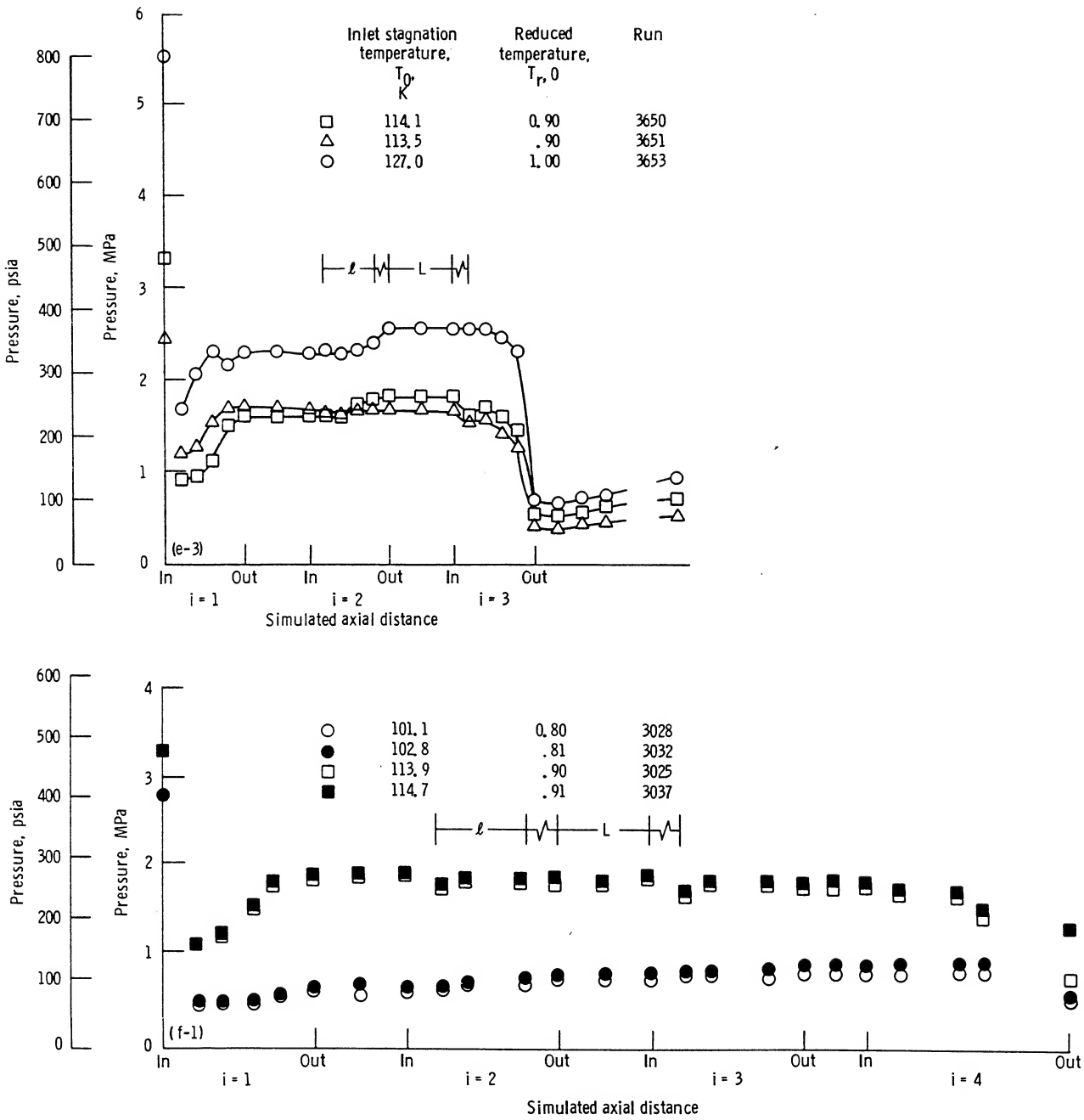

(e) Concluded.

(f) Four Borda inlets at 1.03-cm (0.407-in.) spacing.

Figure 7.—Continued.

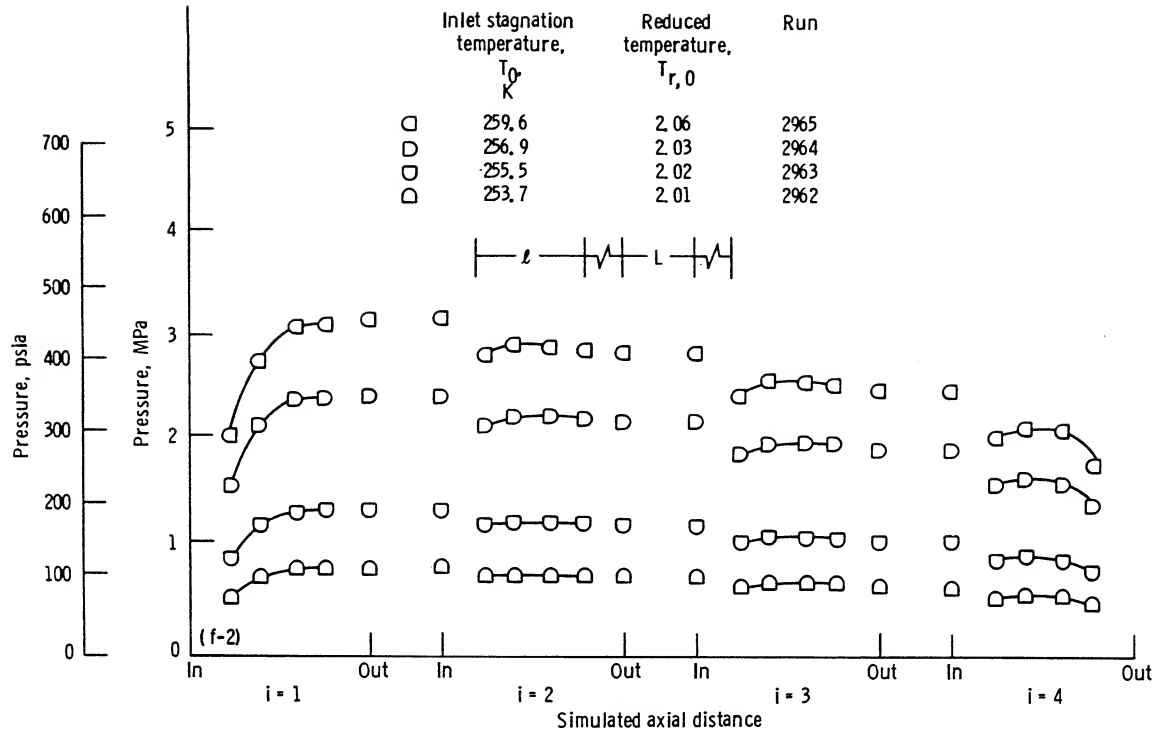

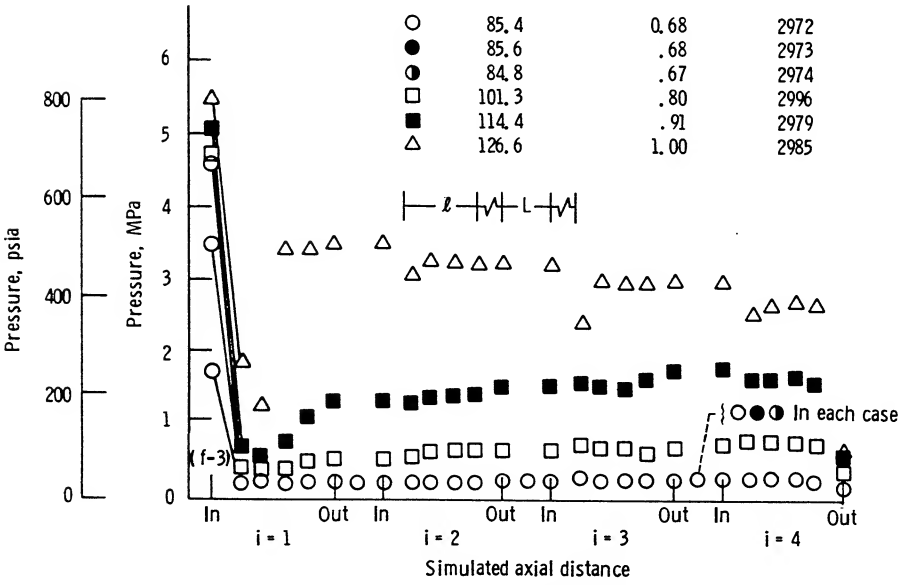

(f) Concluded.

Figure 7.—Concluded.

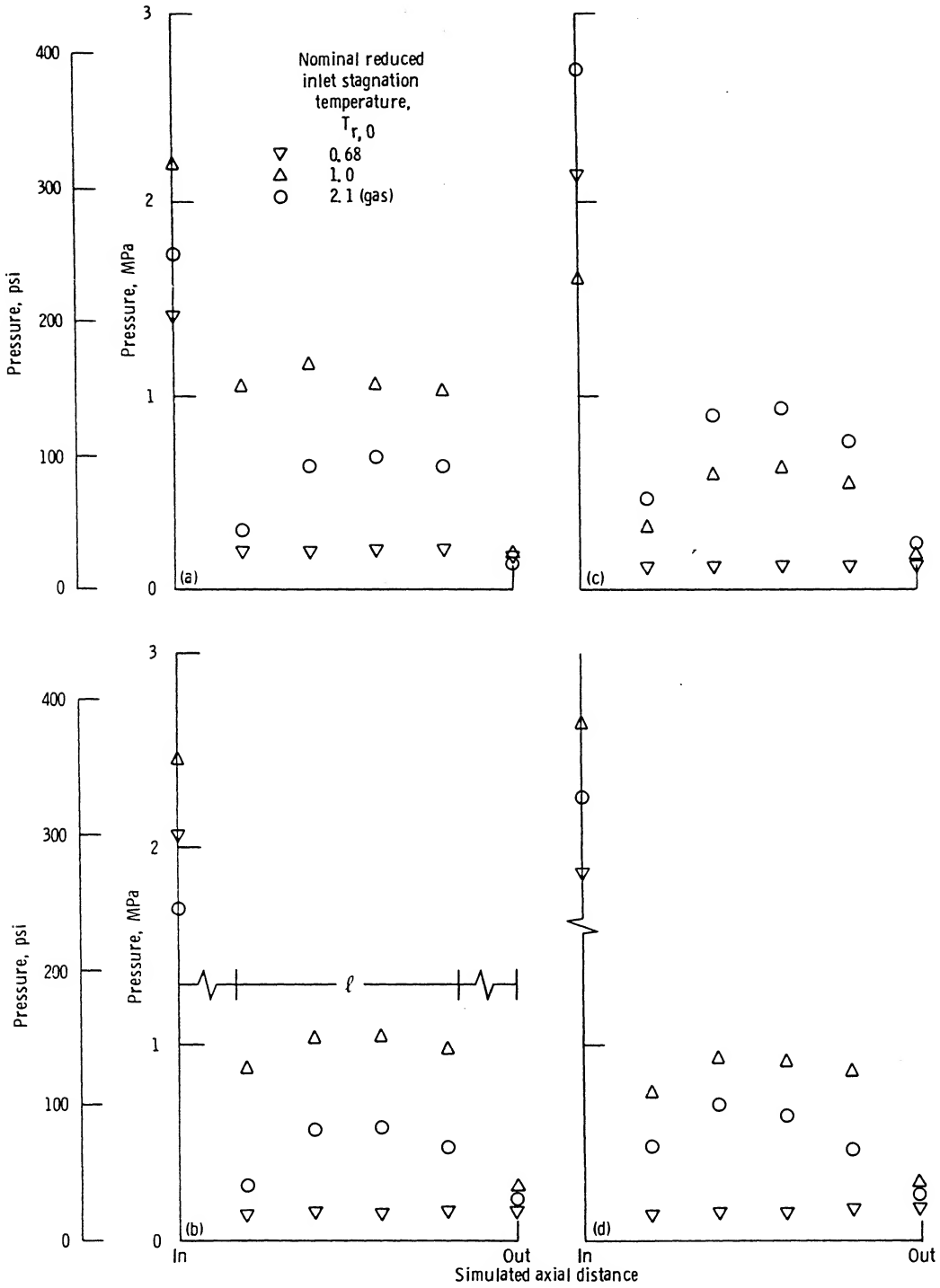

(a) $N=4$.
(b) $N=3$.
(c) $N=2$.
(d) $N=1$.

Figure 8.—Pressure profiles of last inlet of four-, three-, and two-inlet Borda configurations and expected (extrapolated) profile for single Borda inlet.

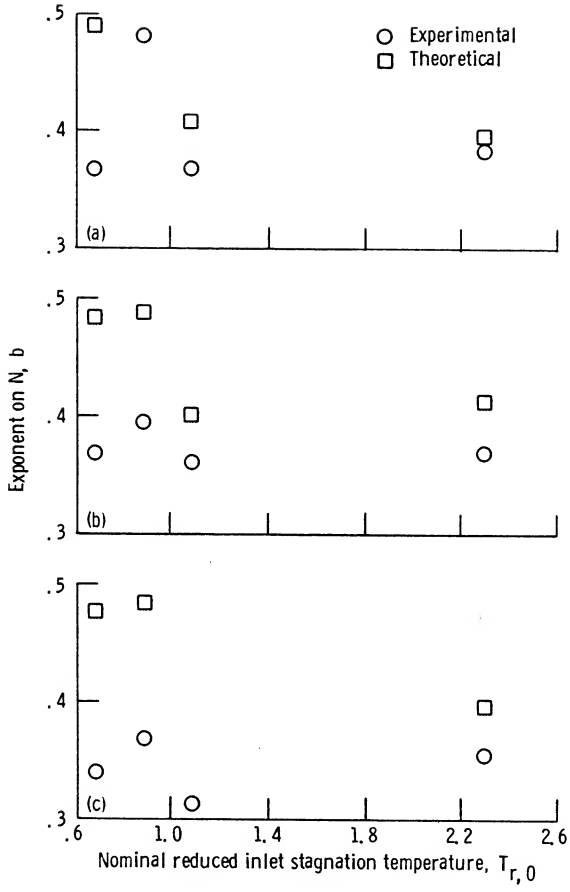

(a) $P_{r,0} = 0.7$.
(b) $P_{r,0} = 1.0$.
(c) $P_{r,0} = 1.5$.

Figure 9.—N^{th}-inlet exponent b as function of reduced inlet stagnation temperature for selected reduced inlet stagnation pressures. ($G_r/G_{r,1} = N^{-b}$.)

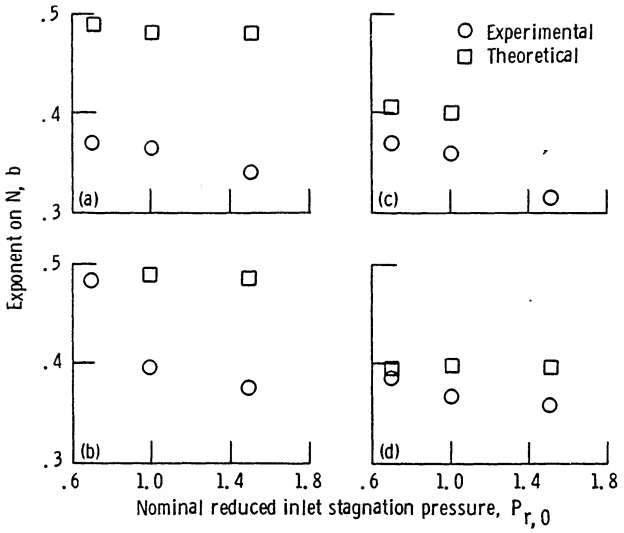

(a) $T_{r,0}=0.68$.
(b) $T_{r,0}=0.9$.
(c) $T_{r,0}=1.1$.
(d) $T_{r,0}=2.3$.

Figure 10.—N^{th}-inlet exponent b as function of nominal reduced inlet stagnation pressure for selected reduced inlet stagnation temperatures. ($G_r/G_{r,1}=N^{-b}$.)

1. Report No.	2. Government Accession No.	3. Recipient's Catalog No.
NASA TP-2390		

4. Title and Subtitle	5. Report Date
Flow Rates and Pressure Profiles for One to Four Axially Alined Borda Inlets	December 1984
	6. Performing Organization Code: 505-32-52
7. Author(s): Robert C. Hendricks and T. Trent Stetz	8. Performing Organization Report No.: E-1979
	10. Work Unit No.
9. Performing Organization Name and Address: National Aeronautics and Space Administration, Lewis Research Center, Cleveland, Ohio 44135	11. Contract or Grant No.
	13. Type of Report and Period Covered: Technical Paper
12. Sponsoring Agency Name and Address: National Aeronautics and Space Administration, Washington, D.C. 20546	14. Sponsoring Agency Code

15. Supplementary Notes

16. Abstract

Choked flow rate and pressure profile data were taken on sequential, axially alined inlets of the Borda type. The configurations consisted of two to four inlets spaced 0.8 and 30 diameters apart. Reference data were taken for the limiting case of a single Borda inlet. At a spacing of 30 diameters the reduced flow rate appeared to follow the simple empirical relation $G_r/G_{r,1} = N^{-b}$, where $G_{r,1}$ is the reduced flow rate for a single inlet; N is the number of inlets; and b, which is weakly temperature dependent, is approximately 0.4. The relation is in reasonable agreement with an analysis of the N-inlet configuration. At a spacing of 30 diameters the pressure profiles dropped sharply at the entrance and partially recovered within each inlet somewhat independently of N. Jetting through the last Borda was common at low temperatures. At a spacing of 0.8 diameter fluid jetting was prevalent at low temperatures for each configuration studied and flow rates were the same as that for a single inlet.

17. Key Words (Suggested by Author(s)): Inlet; Orifice; Sequential flow rate; Pressure profile; Borda

18. Distribution Statement: Unclassified - unlimited
STAR Category 34

19. Security Classif. (of this report)	20. Security Classif. (of this page)	21. No. of pages	22. Price*
Unclassified	Unclassified	32	A03

*For sale by the National Technical Information Service, Springfield, Virginia 22161

NASA-Langley, 1984